NAA-SR-5244
COPY

SNAP 2 REACTOR PUMP DEVELOPMENT PROGRAM (RADIAL GAP PERMANENT-MAGNET PUMP)

AEC Research and Development Report

ATOMICS INTERNATIONAL
A DIVISION OF NORTH AMERICAN AVIATION, INC.

DISCLAIMER

NAA-SR-5244
SPECIAL
PAGES

SNAP 2 REACTOR PUMP DEVELOPMENT PROGRAM (RADIAL GAP PERMANENT-MAGNET PUMP)

By
S. SUDAR

ATOMICS INTERNATIONAL
A DIVISION OF NORTH AMERICAN AVIATION, INC.
P.O. BOX 309 CANOGA PARK, CALIFORNIA

CONTRACT: AT(11-1)-GEN-8
ISSUED: SEPTEMBER 1, 1961

DISTRIBUTION

This report has been distributed according to the category "SNAP 2 Special." A total of 165 copies was printed.

ACKNOWLEDGMENT

The author wishes to acknowledge the contributions to pump design and analyses made by R. S. Baker and G. L. Schmidt.

CONTENTS

TABLE

FIGURES

FIGURES

ABSTRACT

A compact electromagnetic pump utilizing a rotating permanent-magnet with radial gap was developed for possible application to the SNAP 2 reactor coolant system. The pump design objectives were (1) circulation of NaK-78 at 1000°F and 11.2 gpm with a developed pressure of 3 psi; (2) operation at 40,000 rpm; (3) minimum weight and size; and (4) high reliability; one year maintenance free, continuous operation is required.

The performance characteristics of four developmental pump models were measured in a 1000°F NaK test loop and compared with design predictions. The capability of the pump design concept was demonstrated, though further development work is needed to meet the SNAP 2 pump requirements.

A flow capacity of 6.8 gpm of NaK at 1000°F with a developed head of 3 psi was attained at a magnet rotor speed of 40,000 rpm. The weight of this pump is 3 pounds. Reasonable agreement was obtained between the actual pump characteristics and the design predictions.

I. INTRODUCTION

A 3 kw nuclear auxiliary power unit for space exploration and utilization is currently under development for the AEC, at Atomics International, a division of North American Aviation. The SNAP 2 power unit is comprised of a 50 kw liquid metal cooled reactor heat source and a mercury vapor turboelectric power conversion system. The special requirements of a reactor operating in a space environment; minimum weight, completely unattended operation in a zero-gravity, vacuum environment, etc., create problems in the design and operation of the reactor liquid metal coolant system quite different than those experienced in land-based systems. The liquid metal pump, being a major component of this coolant system, is undergoing extensive development work. Responsibility for this program is held by Thompson Ramo Wooldridge, Inc., subcontractor for the SNAP 2 power conversion system. A supplementary program was conducted by Atomics International and is reported here.

The initial objective of the pump development program was to produce a pump to satisfy the SNAP 2 system requirements as follows:

1) Circulate 1000°F sodium at 6.6 gpm and 3 psi head.

2) Operate continuously, maintenance free, for a minimum of 1 year in a zero-gravity environment.

3) Withstand launch environmental conditions: accelerations, vibrations and shock.

4) Conform to the low system weight and size requirements.

In the course of SNAP 2 primary system development work the choice of liquid metal coolant was re-evaluated and NaK-78 was selected to replace sodium. The melting point of NaK-78 is +10°F as compared to 210°F for sodium. The low melting point of NaK will permit charging and startup of the primary system with the coolant in liquid form, and thus materially reduce the problems involved in these procedures. Maintaining the coolant in the liquid state also lessens the possibility of insoluble line plugs forming due to solidification of sodium and sodium oxide mixtures. The use of NaK, however, aggravates the pumping problem since the electrical resistance of NaK, a factor in electromagnetic pump performance, is approximately three times greater than that of sodium.

The main objective of the supplementary pump development program was to establish the feasibility of satisfying the SNAP 2 primary system pump requirements with an electromagnetic type pump. Upon attainment of this objective, which indicated two types of electromagnetic pumps warranting development, the major development effort was carried on by Thompson Ramo Wooldridge (TRW). Partly on the basis of adaptability to their power conversion system design, TRW selected the axial gap permanent magnet pump as the most favorable type and is developing this pump to meet the SNAP 2 requirements.[1] Concurrently, Atomics International continued investigation of the alternative design, the radial gap permanent magnet pump, since the early test results indicated future applicability. The design procedures and test results of this investigation are presented in this report.

II. PUMP DESIGN

A. SELECTION OF DESIGN CONCEPT

The SNAP 2 primary system pump design requirements were:

Working fluid	NaK-78% K
Operating temperature	1000°F
Flow rate	11.2 gpm
Developed pump pressure	3 psi
Rotor speed	40,000 rpm
Minimum weight and size	

1. Mechanical Pumps

The two broad classifications that might be used are positive displacement and centrifugal. Regarding positive displacement design, gear types and their numerous variations are unattractive since the low viscosity of the liquid metals to be used necessitate close running tolerances with the concomitant bearing and wearing surface problems. Work to date has shown no satisfactory metals possessing the requisite frictional and corrosion properties. Additionally a shaft seal is required with ordinary designs thus decreasing the integrity of the coolant system.

Diaphragm designs are inherently low flow units since small movements are necessary to achieve reasonable fatigue life of either the diaphragm or bellows (the latter is more susceptible to fatigue failure). A multiple unit could supply the required flow but only at a severe weight penalty.

Centrifugal types can be subdivided as to the type of sealing system employed to prevent leakage of the liquid metal around the rotating shaft that drives the fluid impeller. Designs that have been used in the past with varying degrees of success are sump, mechanical seal (precision rotating face), freeze seal, and canned rotor types. The sump type is eliminated by the absence of gravity in the ultimate environment. To date, mechanical seals for use with liquid metal have failed to demonstrate adequate integrity and wear resistance to meet the requirements for one year's continuous operation. Both the freeze seal and canned rotor configuration require external cooling which makes them undesirable because of the added complication and the limited radiator area

available. Also, the canned rotor type would entail liquid metal bearing development.

2. Electromagnetic Pumps

The electromagnetic pumps are based on the same principle governing motor operation; namely, a conductor carrying a current in a magnetic field is acted on by a force orthogonal to the electrical and magnetic fields. Electromagnetic pumps can be classified according to the means of producing the current. Consideration in the pump design was given to both conduction and induction electromagnetic pump concepts.

The Faraday type, conduction pumps offer relatively high efficiencies but their requirement of large currents ($\sim$2500 amperes in this application) which necessitates large current carrying members creates a distinct weight disadvantage. An additional drawback is the difficulty of reliably bonding the massive copper bus bars to the high temperature pumping sections, which introduces a low reliability factor to the design.

B. ROTATING PERMANENT-MAGNET PUMPS

The induced current characteristics of induction type electromagnetic pumps permit separation of the hot liquid metal from the pumping power source; the power is transmitted across an air gap to the liquid metal pumping passage, obviating the need for heavy electrical conductors, reducing the material problems, and increasing the design reliability. The varying magnetic field required to induce currents within the liquid metal can be produced by means of polyphase A-C windings, programmed D-C winding, or by direct rotation of a permanent magnet. At the inception of this program reliable high temperature coils were unavailable. The use of windings to produce the magnetic field has the disadvantage of low efficiencies due to the I^2R loss in the windings, associated current source and connecting leads. For a programmed D-C operation, conversion of the available 2000 cps power supplied by the SNAP 2 power conversion system would also cause large energy losses. Also, the reliability of high temperature coils is unknown. It, therefore, appeared that the optimum design could be obtained by the employment of a rotating permanent magnet. To minimize mechanical losses and increase the compactness of the SNAP 2 system, direct coupling of the magnet to the turbine shaft in the combined rotating unit

of the power conversion system was favored. The components of the combined rotating unit, in addition to the primary system pump, are the mercury vapor turbine, mercury pump, and the 2000 cps alternator. The rotating speed of the CRU is 40,000 rpm; direct coupling of the primary system pump fixes its speed, therefore, at 40,000 rpm.

The rotating permanent-magnet pump has two basic forms which can be characterized by the location of the pumping section with respect to the shaft axis and magnetic field as either radial gap or axial gap.

1. Axial Gap Permanent-Magnet Pump

This pump is essentially a centrifugal pump in which the mechanical impeller has been replaced with a magnetic impeller. The fluid enters at the center of the pumping duct and is rotated tangentially by means of a perpendicular rotating magnetic field. Centrifugal force causes the fluid to move radially outward into a volute and through an exit nozzle. The advantage of this permanent magnet pump design is that it permits mounting the magnet rotor on the end of the high speed shaft of the combined rotating unit and, therefore, effectively separates the hot liquid metal from the other components on the shaft. However, Rudenberg predicted in a report to Allis-Chalmers in 1949 that liquid metal in this type of pump would be restrained by eddy-current braking action from flowing radially and that this would seriously impair pumping performance in small size electromagnetic centrifugal pumps.[2] The pump development group at Thompson Ramo Wooldridge selected this pump concept as most favorable of any considered on the basis of their analysis of pump efficiencies and overall system requirements.

2. Radial Gap Permanent-Magnet Pump

This pump utilizes a permanent magnet in the form of a cylinder which is mounted directly upon the high speed shaft. The cylinder is magnetized so that the flux lines pass radially outward through an annular gap containing the pumping duct to a high permeability laminated iron cylinder which serves as the magnet flux return path. The rotating magnetic field causes the liquid metal within the duct to rotate concentrically; spiralling the pumping duct causes the fluid to flow through the pump. This concept warranted development because of simplicity in construction and favorable test results obtained with a prototype

model. Four models of the radial gap permanent magnet rotor pump were built and tested. These pump models are designated in this report as Mark I, II, III, and V. The Mark IV pump was designed, then revised prior to fabrication. The revised design (Mark V) was built and tested.

C. DESIGN PROCEDURE

The basic design equation for calculating the pressure developed by the traveling magnetic field of a permanent-magnet rotor pump was derived by R. S. Baker who utilized a method similar to R. Rudenberg's analysis for the derivation of the equation for the braking force in an eddy current brake.[3,4] The pump design equation is as follows:

$$P = \frac{(V_{syn} - V_\ell)\lambda h}{4\rho\tau(68,944)} \left\{ \frac{\frac{\lambda}{\tau} + \frac{\tau}{\lambda}}{\left[\frac{4(V_{syn} - V_\ell)\delta_1\lambda}{\rho\delta}\right]^2 + \left[\frac{\lambda}{\tau} + \frac{\tau}{\lambda}\right]^2} \right\} B_G^2 \qquad \ldots(1)$$

To clarify the terms used in the above expression, a radial gap permanent-magnet rotor pump is shown schematically in Figure 1.

Pressure losses occur within the permanent magnet rotor pump due to hydraulic losses, within the pumping section and at inlet and exit ends, and to electromagnetic losses. The latter are due to the force produced by the axial motion of the fluid conductor within the magnetic field; this force opposes the axial fluid motion.

The hydraulic losses of the pumping section are readily determined experimentally with measurements performed on a pumping section mockup in a water test loop. The water test data are then converted by the principles of model theory to provide pressure drop data under actual pump operating conditions. Several inlet and exit pump nozzle and pump annuli designs were tested in the water loop in order to determine a design with minimum hydraulic losses. Use of the standard equations to calculate fluid friction and expansion-contraction losses will produce only approximate pressure drop information because of the complex geometries involved.

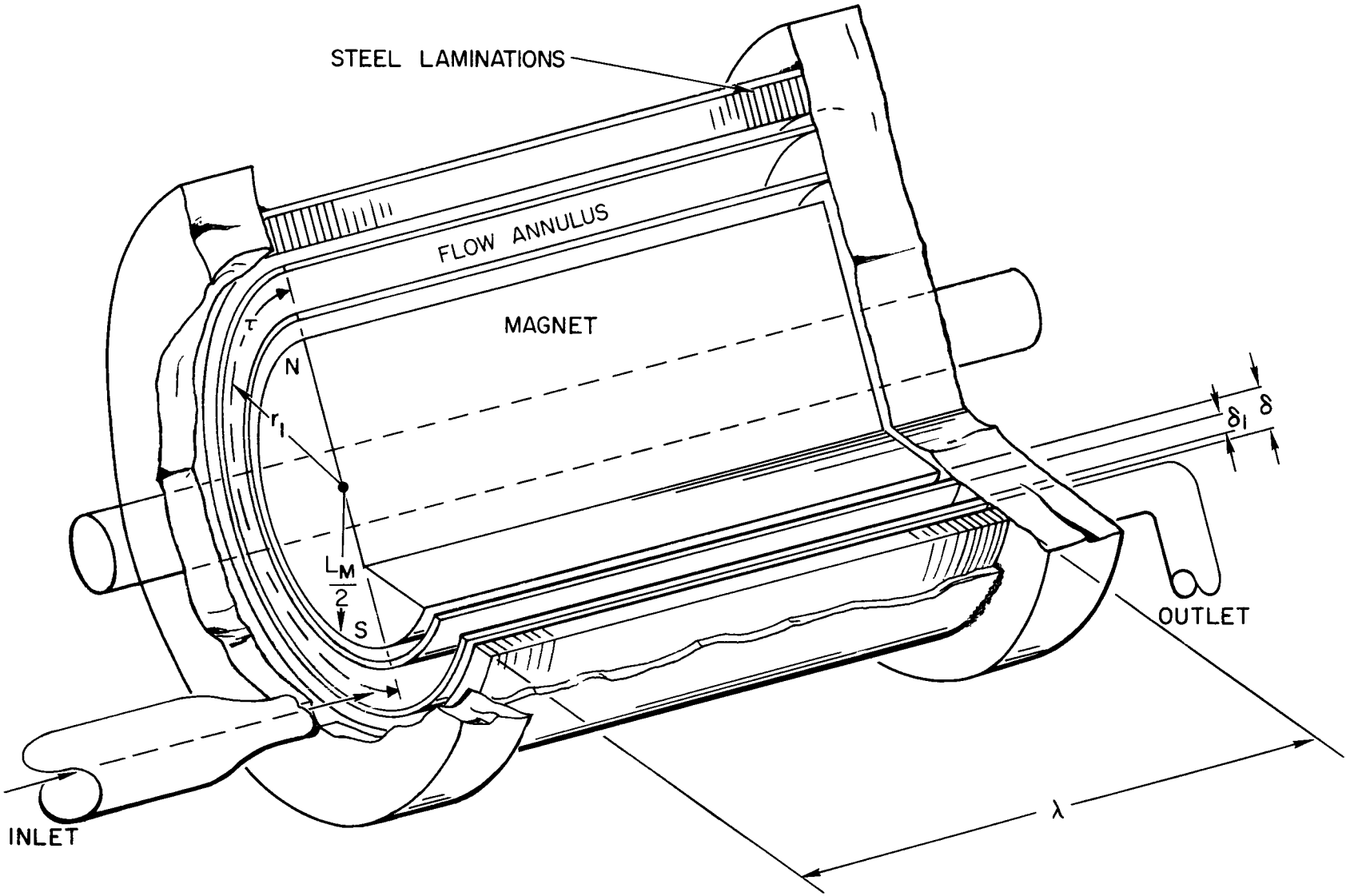

Figure 1. Basic Design of Rotating Permanent-Magnet, Radial Gap Pump

The electromagnetic losses can be determined by use of the following equation:[5]

$$P_{axial} = \frac{V_{\ell a} \tau B^2}{2\rho(68,944)} \left\{ \frac{\frac{\lambda}{2\tau} + \frac{2\tau}{\lambda}}{\left[\frac{4V_{\ell a}\delta_1}{\rho\delta}\right]^2 + \left[\frac{\lambda}{2\tau} + \frac{2\tau}{\lambda}\right]^2} \right\} \quad \ldots (2)$$

The theoretical pressure developed by the pump is then obtained as follows:

$$P_{net} = P - P_{axial} - P_{hydraulic}$$

Additional power losses occur in the pump due to resistance heating, friction and windage. Eddy currents induced within the wall of the pumping section and the stationary layer of fluid adjacent to the wall result in resistance heat losses. The losses within the wall can be minimized by utilizing materials having high electrical resistivity and by making the wall as thin as structural requirements permit.

Additional resistance heating losses are produced in the iron laminations which form the flux return path. These losses are minimized by electrical separation of the individual laminations with mica insulators.

Losses due to friction are minimized by careful bearing design. Windage losses will be negligible in the space operating environment. During ground testing the combined friction and windage losses are determined experimentally.

Sample calculations of developed pump pressures under shutoff and flow conditions are presented in the Appendix.

Additional factors enter into the design of the SNAP 2 pump; these factors, the design values and their major significance in design are tabulated below:

Factor	Design Value	Major Significance in Design
Pump weight	3 lb maximum	Limits size of magnet
Critical speed of CRU	> 40,000 rpm	Limits size of magnet to 1.5 in. long by 1.5 in. diameter (Ref. 6)
Rotor stresses at 40,000 rpm		Affects selection of magnet material and need for magnet support

Factor	Design Value	Major Significance in Design
Magnetic gap	Minimum size	Limits size of pumping section and magnet support sleeve thickness
Launching forces	10 g	Governs thickness requirements of pumping section wall

Mark I, II, and III pumps were partially based upon the above design factors since they were designed to determine the feasibility of the pump concept and to provide data on pump performance as affected by pumping section and magnet characteristics. The Mark V pump design, however, was prepared with close attention to all the design factors.

III. PUMP DESCRIPTIONS

The four developmental models of the radial gap permanent-magnet rotor pump conformed to the basic design shown in Figure 1. The major differences in the pump designs were in the pumping sections and the magnet dimensions. The pumping sections were all fabricated with 304 stainless steel.

A. MARK I PUMP

The pump assembly is illustrated in Figure 2. The rotor consisted of five cast Alnico V 1-1/2 in. by 3/8 in. discs stacked in a stainless steel housing to form a magnet 1-7/8 in. long and 1-1/2 in. diameter. The housing was designed to contain the magnet material on the conservative assumption that the Alnico V contributed zero strength. The configuration of the pumping section is shown in Figure 3. It contained a helical vane which made two complete turns through the flow annulus. Dimensions of the annulus were 2 in. long by 0.170 in. thick. The fluid entered and exited the annulus in a direction parallel to the rotor axis. The entrance and exit sections were made small in order to provide the shortest distance feasible between the high speed rotor bearings. This was deemed desirable because of the uncertainty in the initial tests regarding the stability of the high speed rotor assembly. Characteristics of this design were the large hydraulic pressure losses due to the abrupt changes in flow cross sections and the presence of high velocity flow sections. Conventional single-shielded grease packed bearings were used for the high speed rotor.

B. MARK II PUMP

The Mark II pump is shown in Figure 4. The chief modification was the increase in entrance and exit sections to reduce the internal hydraulic pressure losses. The fluid entered and exited the flow annulus via end chambers in a direction normal to the rotor axis. Two pumping section configurations were used in the test runs. The first configuration consisted of a single spiral vane through the flow annulus. The annulus was 3.25 in. long and 0.170 in. thick. After several tests, the inner wall of the annulus collapsed. Insufficient data were obtained with this configuration to permit an analysis to be made. The pumping section in the second configuration contained two parallel helical vanes, each making a single complete turn through the flow annulus.

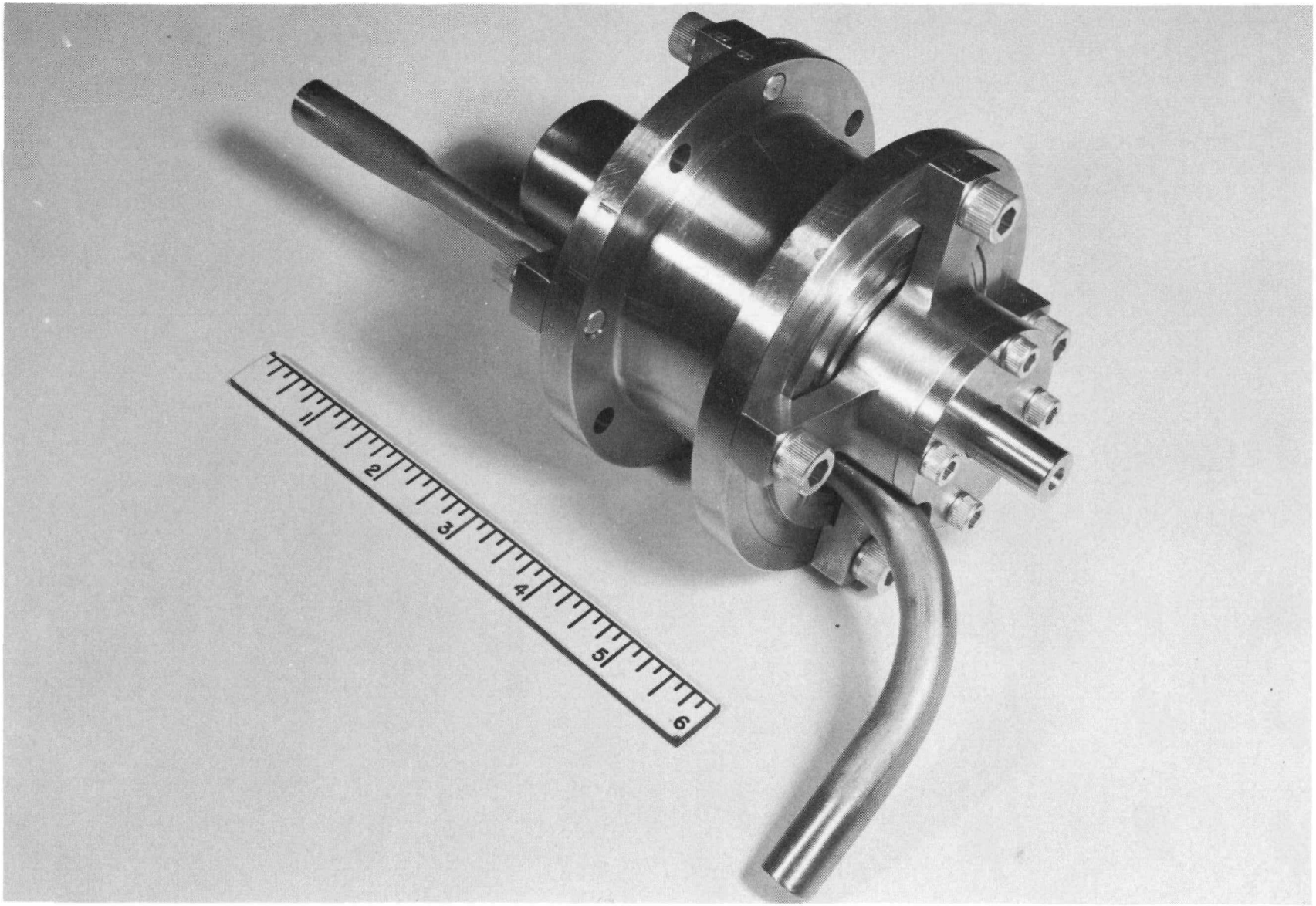

Figure 2. Mark I E-M Pump

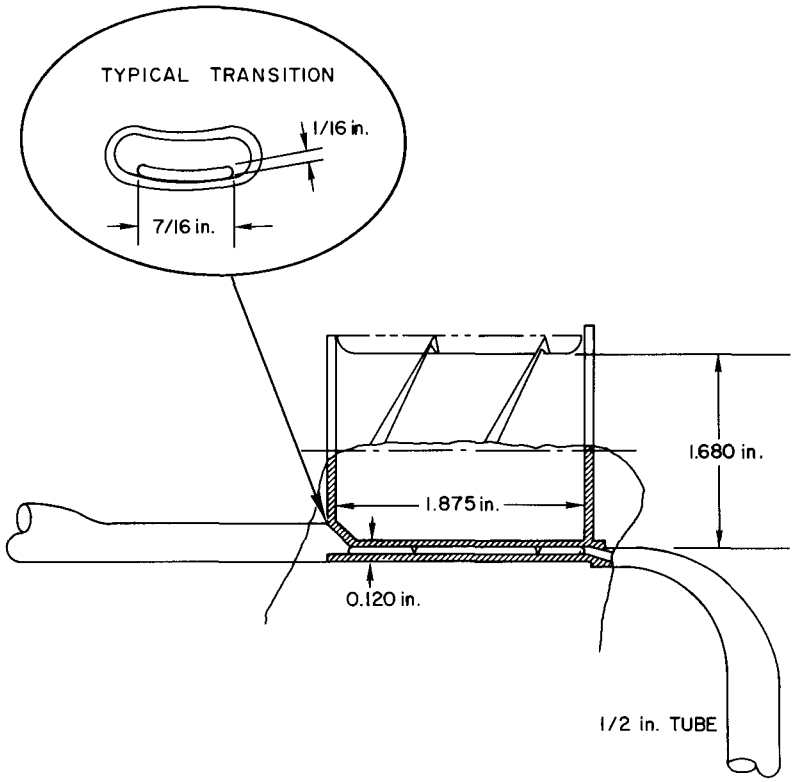

Figure 3. Mark I Pump Flow Annulus

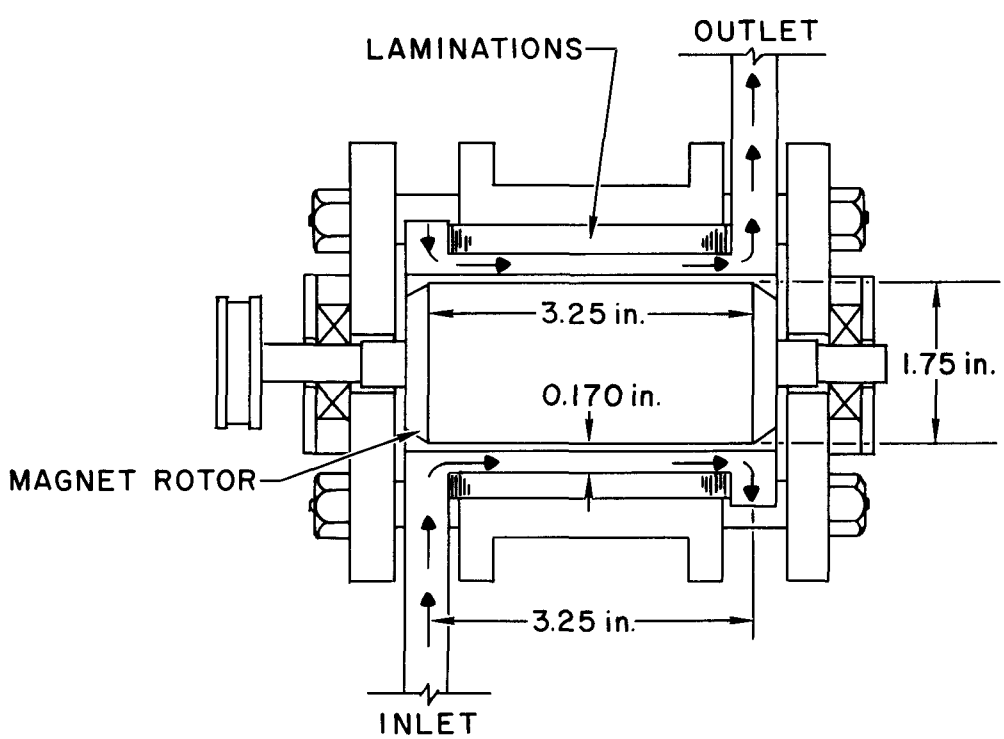

Figure 4. Mark II E-M Pump

The magnet assembly consisted of two 1.75 in. diameter Alnico V magnets placed within a sleeve to provide additional strength for the high rotor speeds. The magnets were magnetized normal to the axis of rotation and were placed within the sleeve with similar poles aligned in the same direction. The overall magnet length was 3.25 in.

The pump performance tests indicated that the design flow and developed pressure requirements, then based upon 6.6 gpm of sodium and 3 psi, would be exceeded at the design speed of 40,000 rpm. The weight of this pump, however, greatly exceeded the design requirements; 3 pounds had been set as an objective and this pump weighed 8 pounds. The pump design was, therefore, modified in an effort to meet the weight requirement.

C. MARK III PUMP

The Mark III pump configuration is shown in Figure 5. Size and weight were the major differences between the Mark II and Mark III pump designs. The Mark III pumping section was 2.0 in. long and 0.17 in. thick. The flow annulus contained two parallel, helical vanes, each making slightly less than one complete revolution. The vane angle was 45 degrees. The vanes and fluid inlet and outlet end chambers are shown in Figure 6. The pump rotor assembly contained an Alnico V magnet supported by an interference fit steel sleeve. The magnet dimensions were 1.15 in. long and 0.935 in. diameter. This pump inclusive of the rotor assembly weighed 4 pounds.

The performance of this pump was well below expectations. The poor performance was attributed to the small size of the magnet. An additional factor in subsequent pump design work was the change in reactor system coolant to NaK-78, which was made approximately at this stage of the pump development program. The higher electrical resistivity of the NaK-78 in addition to the need for a higher flow rate, 11.2 gpm, made the SNAP 2 primary system pump requirements even more stringent. Based upon results to date, a revamping of the pump design seemed necessary.

D. MARK V PUMP

The Mark V pump, shown in Figure 7, incorporated a major change in pumping section design. The vaned pump annulus, used in the previous pump

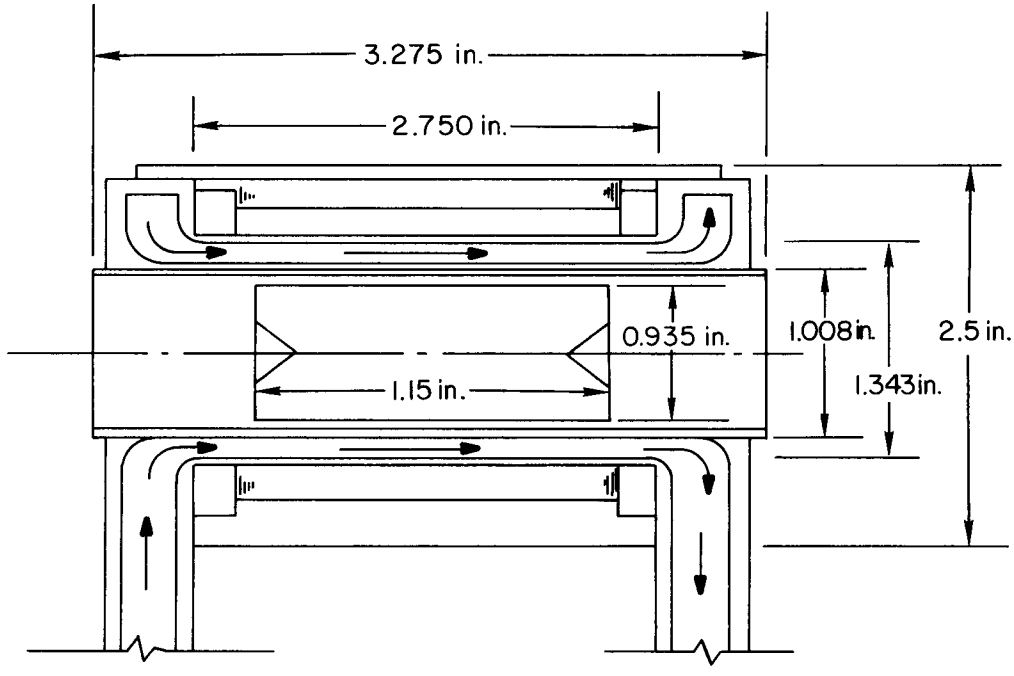

Figure 5. Mark III E-M Pump

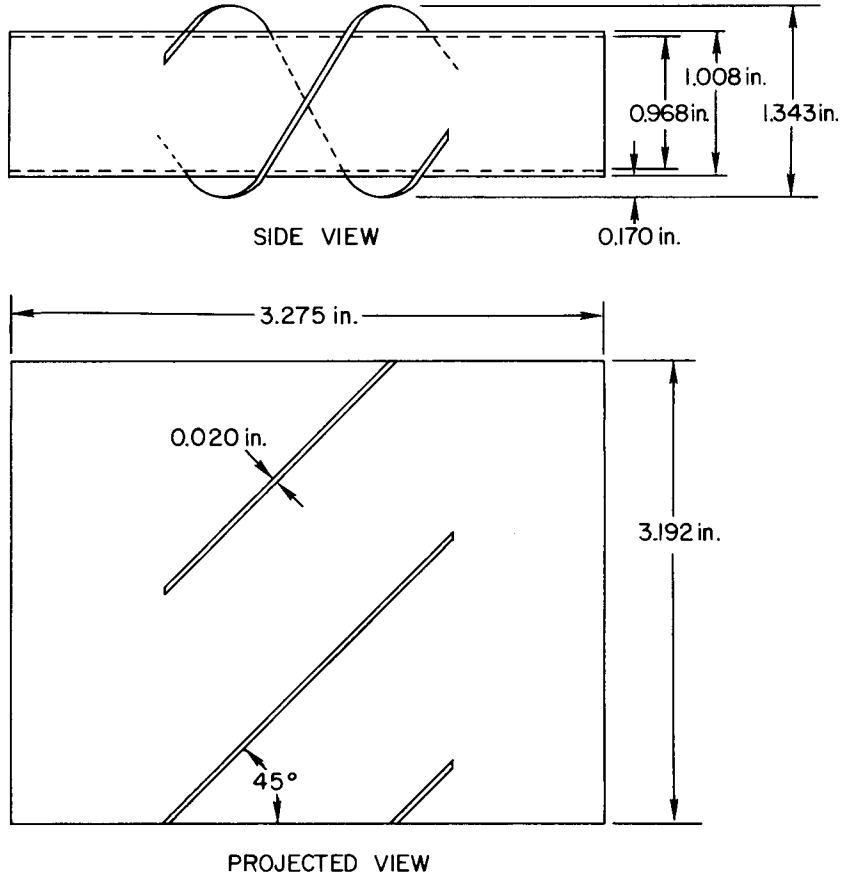

Figure 6. Mark III Pump Flow Annulus

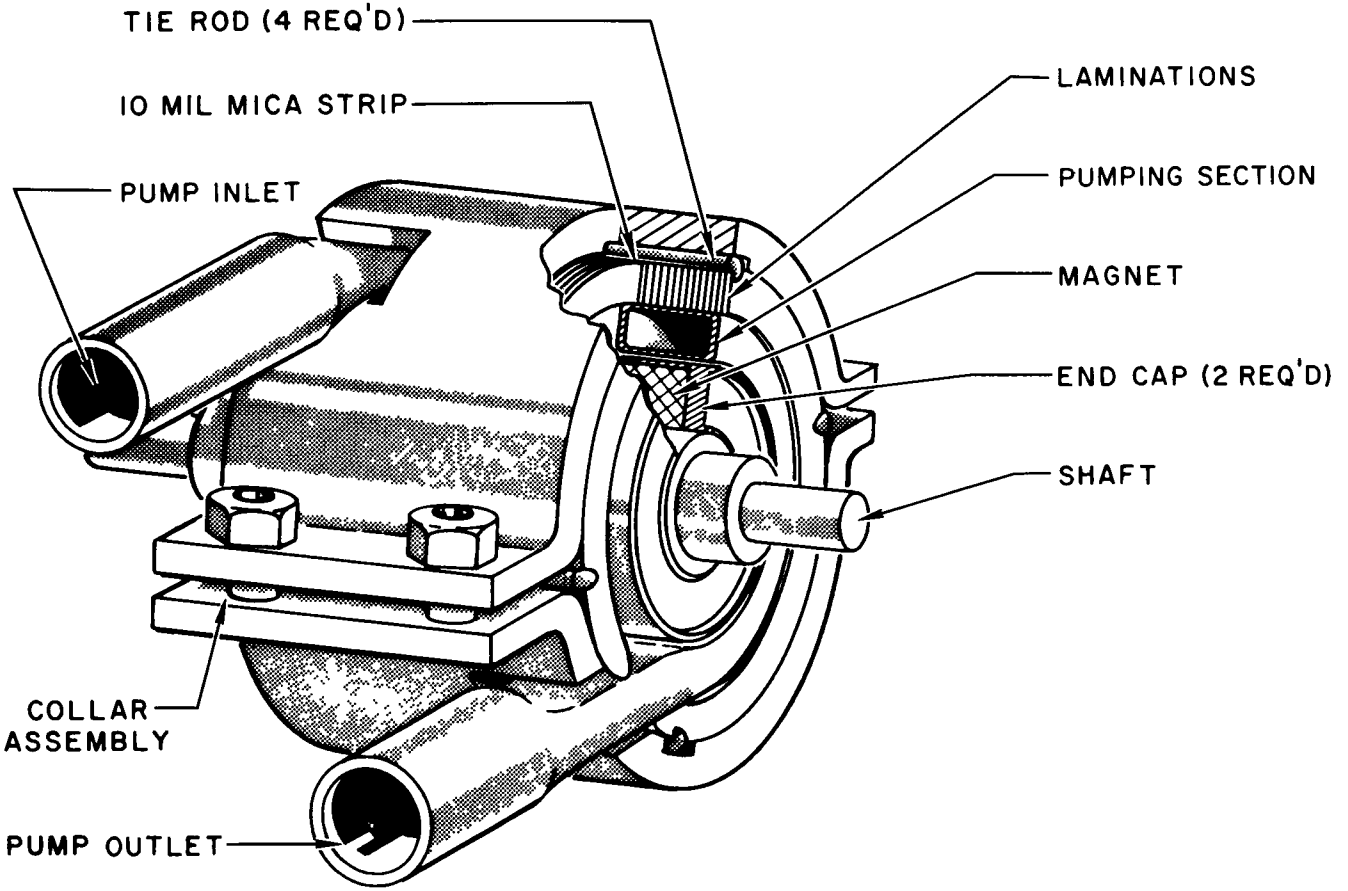

Figure 7. Mark V E-M Pump

models, was replaced by a helically coiled rectangular flow tube. This modification provided continuity of flow direction, minimum change in flow area at pump inlet and outlet, and a more well defined flow channel. Details of the pumping section are shown in Figure 8. The rotor assembly was 1.50 in. long and 1.46 in. diameter. Two magnet materials, Alnico V and Alnico VI were tested. The Alnico VI magnet, having adequate tensile strength, was used without a supporting sleeve. The pump, including the rotor assembly, weighed 3 pounds.

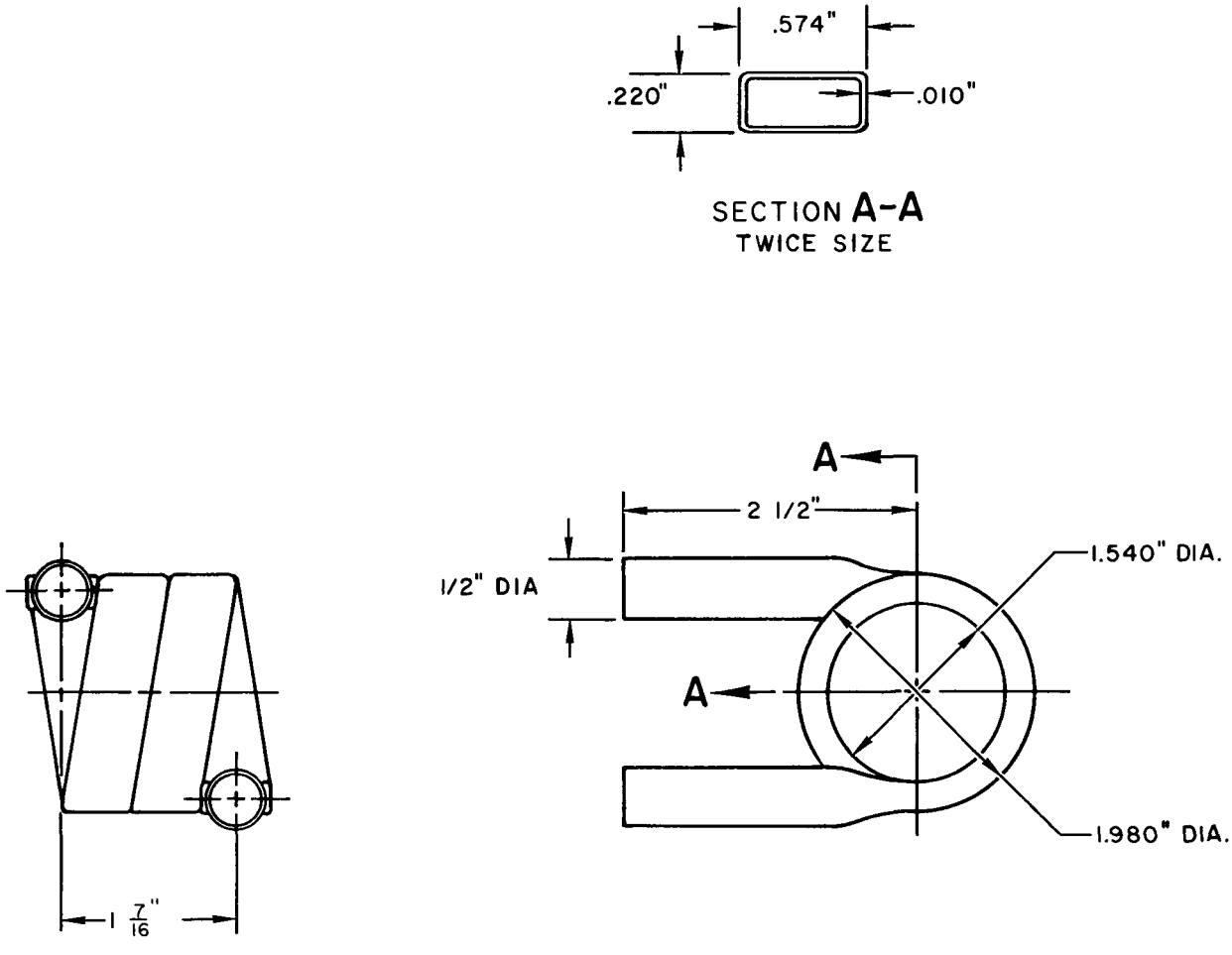

Figure 8. Mark V Pump Flow Duct

IV. TEST APPARATUS

The test apparatus consisted primarily of a liquid metal test loop, a high speed pump drive mechanism, and instrumentation to measure and control the several parameters entering into evaluation of the permanent-magnet rotor pump performance.

A. TEST LOOP

A flow diagram of the test loop is shown in Figure 9, and a photograph of the test loop during the Mark V pump test is shown in Figure 10. The loop was a completely welded assembly comprised of type 304 stainless steel, 1 in. diameter, schedule 40 piping. The loop was made up of the following major components: test pump, control valve, magnetic flowmeter, diffusion cold trap, combined "J" tube liquid level indicators and surge tanks, and combined drain and fill tank. System pressure was controlled with helium cover gas. Resistance heaters strapped to the loop piping were used to bring the system temperature to the operating level in the range of 700 to 1000°F. The test loop was thermally insulated with asbestos. All valve adjustments and instrument readouts were made remotely.

B. PUMP DRIVE MECHANISM

The need for a pump shaft speed of 40,000 rpm to simulate the design condition created a problem in selection of a pump drive mechanism. Operation of test pumps Mark I, II, and III utilized an electric motor drive in association with reduction gears and drive pulleys, but serious limitations were encountered. The rapid wear and frequent failure of the drive belts prevented sustained operation of the pump and hampered experimental test runs. Also, accurate measurement of actual shaft power input was impossible due to the nondeterminable losses in the drive mechanism.

Availability of high speed electric motors (grinder motors) permitted direct drive operation of the Mark V pump at the design speed of 40,000 rpm. The drive used was a 1.42 hp, 54,000 rpm, 2 phase induction motor directly coupled to the pump shaft. Speed adjustment was obtained in continuous increments from 15,000 to 40,000 by means of a frequency converter power supply rated at 220 volts input 3ϕ and variable voltage output.

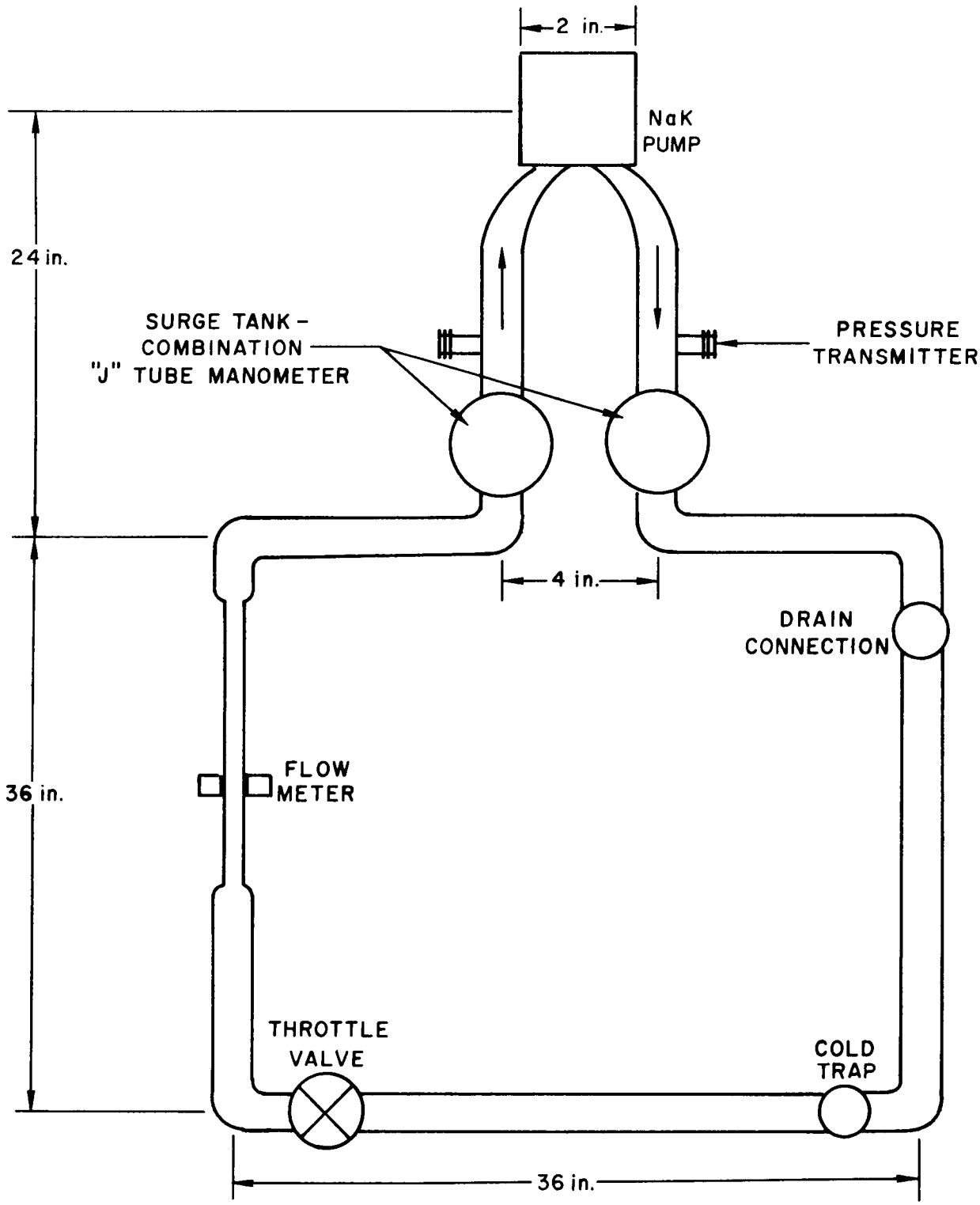

Figure 9. Flow Diagram of Pump Test Loop

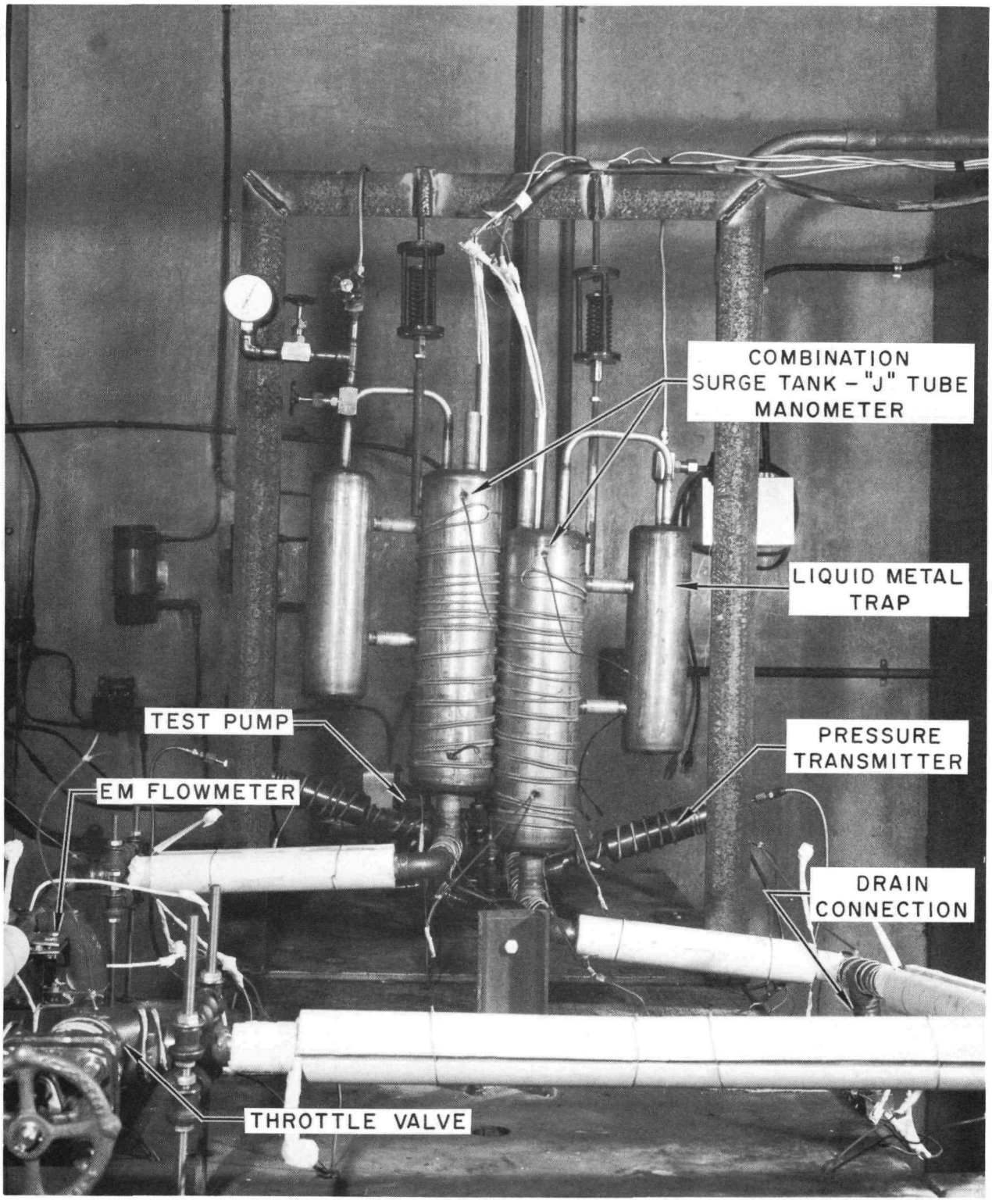

Figure 10. Pump Test Loop

C. INSTRUMENTATION

1. Developed Pump Pressure

Pump pressures at suction and discharge ends were determined by use of high temperature pressure transducers with pneumatic transmission to a manometer containing either mercury or carbon tetrachloride. These pressures were checked satisfactorily with "J" tube level indicators in association with pneumatic transmission to a mercury filled manometer. Differential pressure measurement accuracy was ± 1%.

2. Flow Rates

A calibrated liquid metal magnetic flowmeter utilizing a permanent magnet was used to measure the system flow rates. The D-C signal output was recorded on an EMF potentiometer type recorder; flow measurement accuracy was ±1%.

3. System Temperature

The temperature of the liquid metal was determined with chromel-alumel thermocouples attached to the surface of the loop piping at several locations proximate to the test pump. A potentiometer type multipoint temperature indicator was used for temperature readout; accuracy was ±1%.

4. Power Input

Power input to the Mark V pump drive motor was measured with a dynamometer type 50-800 cycle wattmeter. Accuracy of the power reading was ±3/4%. A calibration was made of the high speed direct drive motor with use of a dynamometer in order to determine the actual power output of the motor as a function of power input. This calibration curve is shown in Figure 11.

The power inputs to the drive motor for Mark I, II, and III were measured with a wattmeter. The aforementioned nondeterminate transmission losses, however, reduced the significance of this measurement.

5. Pump Speed

Pump rotating speed was measured with a tachometer utilizing an optical pickup and readout on a frequency meter. A vibrating read tachometer was employed on tests of Mark I-III. However, the hazards attendant to the required direct readout of this instrument made it undesirable. Accuracy of the optical tachometer was ±1%.

6. Magnet Flux Density

Flux density measurements of the magnet were made (prior to and after operation of the test pump) with a gaussmeter utilizing a bismuth probe. The magnets were stabilized by exposing them to the operating condition of the pump through several temperature cycles produced by gradually heating and cooling the system between 1000°F and ambient; subsequent change in magnetic strength caused by normal operating conditions and standard handling procedures was negligible. Accuracy of the gaussmeter was ±1%.

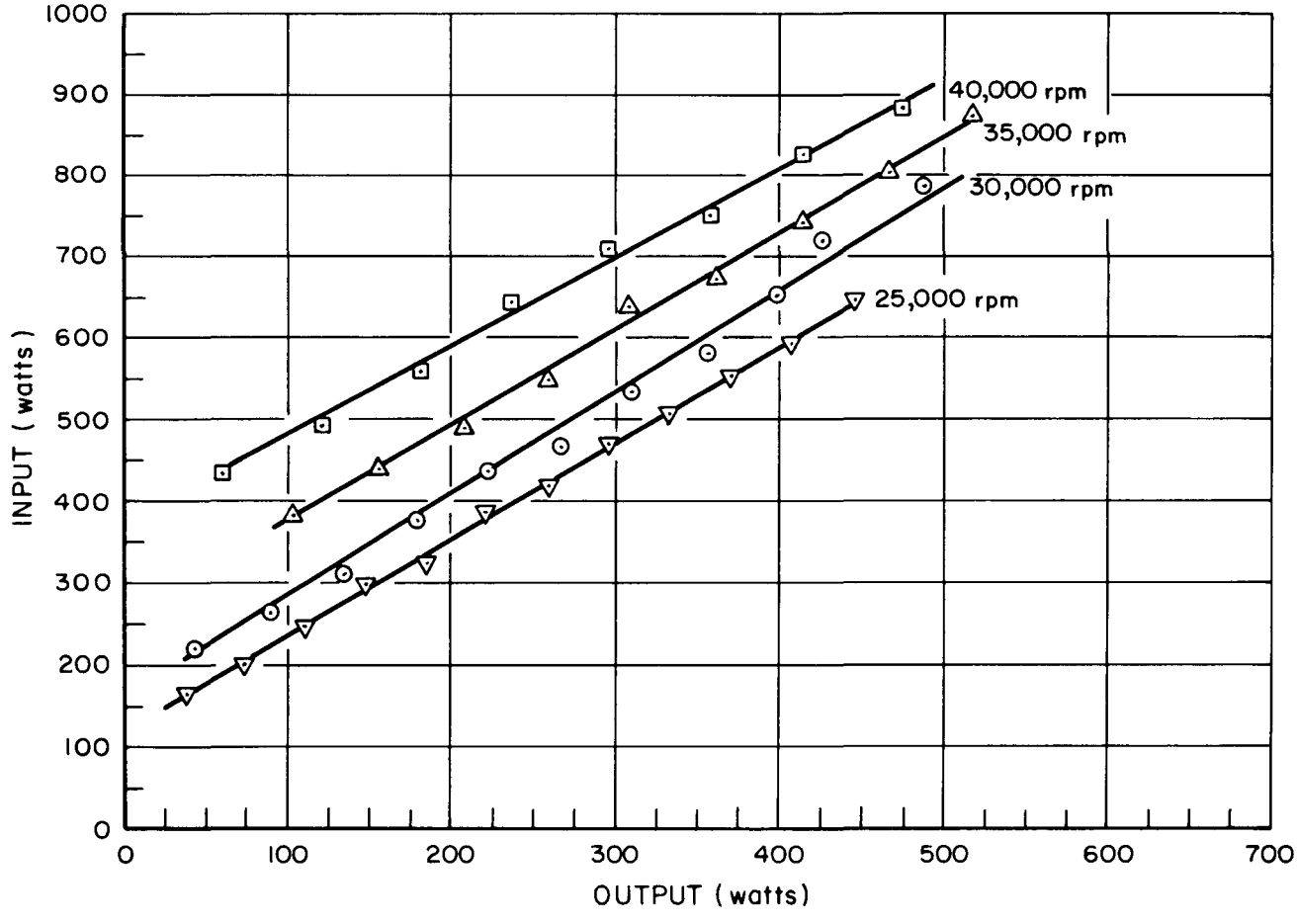

Figure 11. Calibration Curve of Mark V Pump Drive Motor

V. PROCEDURES

A. PUMP PERFORMANCE TESTS

Head-capacity data were obtained for the four permanent-magnet rotor pumps in the pump test loop. Tests were performed with sodium and NaK-78; test procedures differed for the two liquid metals only in that loop preheating was required prior to charging of the system with sodium. The following procedure was used in the testing of the Mark V pump and was generally typical of all the pump tests. The test loop was evacuated to 50 microns, charged with NaK-78, then filled with helium cover gas to a system pressure of ~6 psig. The test pump was then started at a relatively low rotor speed (15,000 rpm) to circulate the NaK. The NaK temperature was elevated to operating level (usually 1000°F) by resistance heaters attached to the loop piping. The diffusion cold trap was utilized to maintain the oxide concentration at a low level. Test runs were made at constant pump rotor speed, NaK flow rate and temperature. Measurements were taken of the following:

1) Pump rotor speed

2) NaK flow rate

3) NaK temperature

4) Differential pressure across the pump.

By adjustment of the flow control valve, differential pressure measurements were obtained over a range of flow rates at constant pump speed and system temperature. This procedure was repeated over a range of pump speeds and additional parameters as follows:

Pump speed	15,000 to 40,000 rpm
Fluid temperature	700 to 1000°F
Magnet flux density	1400 to 1800 gausses

B. HYDRAULIC LOSSES

The internal pressure losses of the four test pumps were measured in a water loop, which permitted measurement of pumping section hydraulic losses prior to incorporation of the pumping section design into the pump assembly.

By application of the principles of model testing,[7] which require geometric and dynamic similarity between the model and the prototype, the pump pressure losses measured in the water system were converted to losses in the liquid metal system. Dynamic similarity was obtained by making the Reynolds number of the model equal to the Reynolds number of the prototype. The following relationships, based upon the Darcy equation for head loss due to pipe friction, are employed to convert the water test data.

$$(\Delta P)_w = \left(f \frac{L}{D} \frac{V^2}{2g} \frac{\rho}{144} \right)_w$$

$$(\Delta P)_m = \left(f \frac{L}{D} \frac{V^2}{2g} \frac{\rho}{144} \right)_m$$

where subscripts w and m denote water and liquid metal, respectively. For similar geometry and equal Reynolds numbers:

$$\left(\frac{fL}{2gD} \right)_w = \left(\frac{fL}{2gD} \right)_m$$

therefore,

$$\frac{(\Delta P)_w}{(V^2 \rho)_w} = \frac{(\Delta P)_m}{(V^2 \rho)_m}$$

also

$$\left(\frac{DV\rho}{\mu} \right)_w = \left(\frac{DV\rho}{\mu} \right)_m$$

$$\frac{V_w}{V_m} = \frac{\nu_w}{\nu_m}$$

therefore,

$$(\Delta P)_m = \Delta P_w \frac{(\nu^2 \rho)_m}{(\nu^2 \rho)_w} .$$

For water at 80°F and NaK-78 at 1000°F

$$\Delta P_m = 0.051 \Delta P_w .$$

The hydraulic losses for the test pumps are shown in Figure 12.

C. MEASUREMENT OF MAGNET FLUX DENSITY

The procedure used in this experimental program for determining the flux densities of the several magnets employed was to measure the flux density of each magnet before and after the series of test runs with a gaussmeter. The measurements were performed outside of the pump assembly after the magnets had been thermally cycled to include the effect of temperature upon the magnitude of flux density under pump operating conditions. Since the flux density under dynamic conditions may be different from the static measurement, a dynamic measurement was made by the use of a one-turn coil installed in the air gap between the rotor and the pumping section as shown in Figure 13. The electromotive force developed by the rotating magnetic field was recorded with a vacuum tube voltmeter, the flux density was then calculated by application of the standard equation:

$$E_A = B_A \ell v$$

where

E = induced emf (volts)

B_A = average magnetic flux density (gausses)

ℓ = length of coil (cm)

v = velocity of rotating magnetic field (cm/sec)

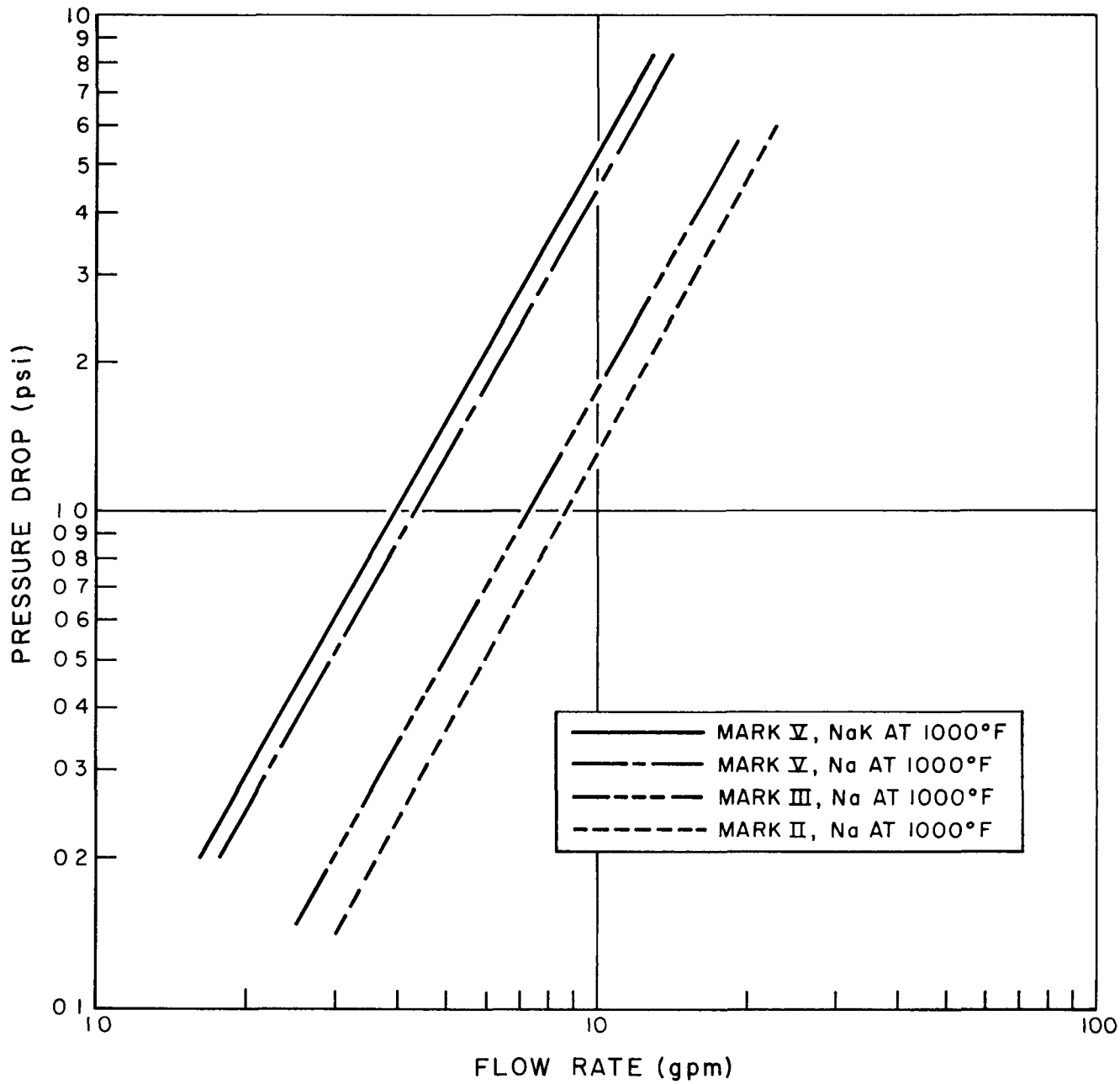

Figure 12. Hydraulic Losses of the Radial Gap E-M Test Pumps

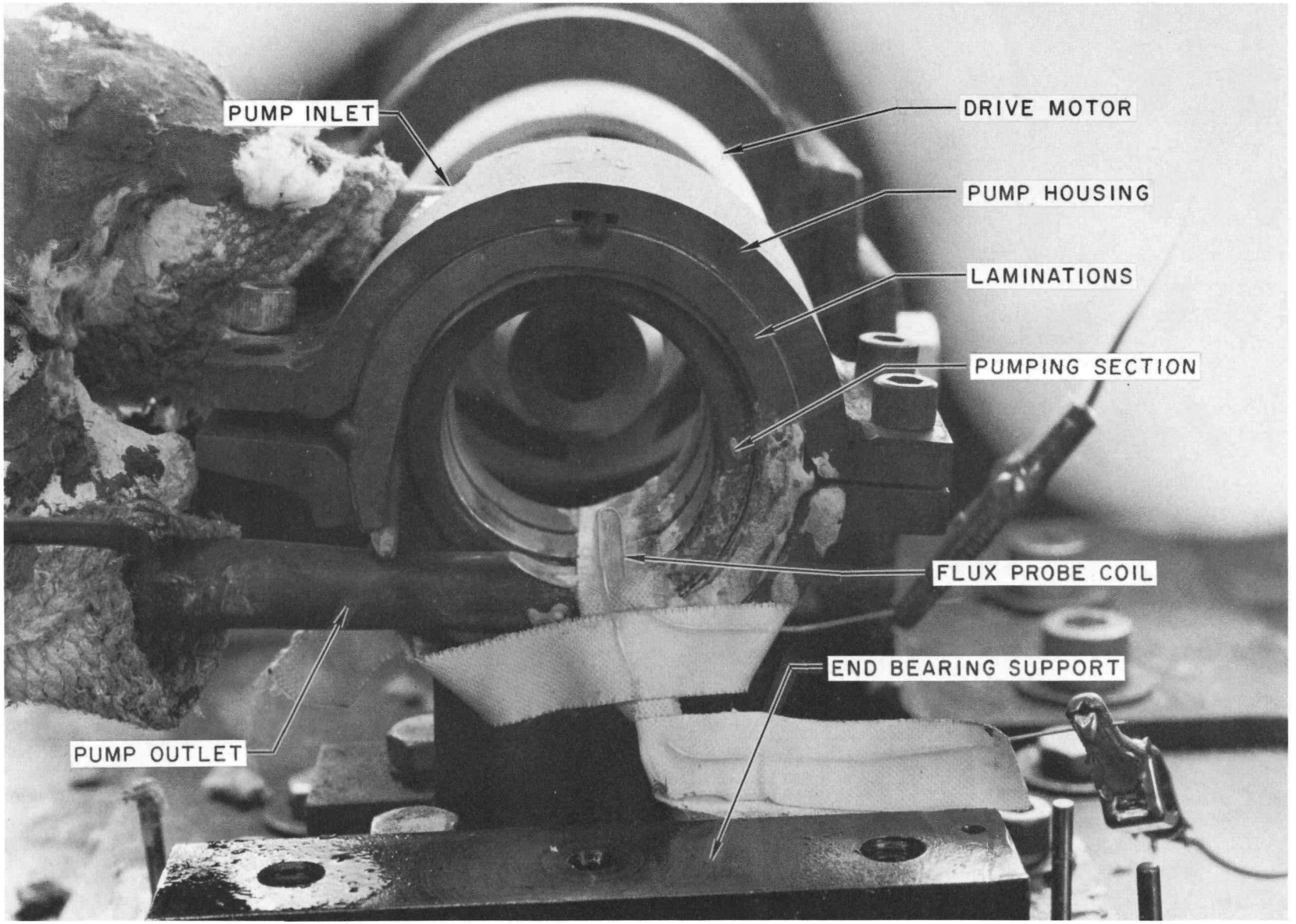

Figure 13. Assembly for Dynamic Measurement of Magnet Flux Density

Taking into account the sinusoidal flux distribution in the direction normal to the rotor axis:

$$B_G = \frac{\pi}{2} B_A$$

where

B_G = peak magnetic flux density

The following data were obtained with the Alnico V magnet used in testing of the Mark V pump:

1) Static measurement

Final flux density	1550 gausses

2) Dynamic measurements at 1000°F

Rotor Speed (rpm)	Magnet Flux Density - B_A (gausses)
15,000	1606
25,000	1628
30,000	1625
35,000	1531
40,000	1520

Reasonable agreement was obtained between the static and dynamic measurement. The decrease in B_A observed with increasing rotor speed can be attributed to the effect of armature reactance.

D. DETERMINATION OF PUMP EFFICIENCY

Efficiencies for the Mark V pump were determined as follows:

$$\eta = \frac{W_o}{W_i} \times 100$$

where

η = efficiency (%)

W_o = fluid power output (watts)

W_i = shaft power input (watts).

Determination of fluid power output:

$$W_o = 0.435PQ \text{ (watts)}$$

where

P = developed pressure (psi)

Q = flow rate (gal/min).

Determination of shaft power input: The pump shaft power input was obtained from a calibration of the pump drive motor. The Mark V pump drive motor was calibrated with a dynamometer to determine the output shaft power as a function of input power, shown in Figure 11. During each test run the power input to the drive motor was measured with a precision wattmeter; the pump shaft power input was then obtained from the calibration curve.

The combined bearing friction and windage losses for the pump rotors were determined by measurements of the power required to rotate a dummy (non-magnetic) rotor. The windage losses in the space environment will be negligible, but the friction losses will still occur. Since there were no practical means of isolating the windage losses, the combined losses are included in the value of shaft power input. The combined losses for the Mark V pump are shown in Figure 14.

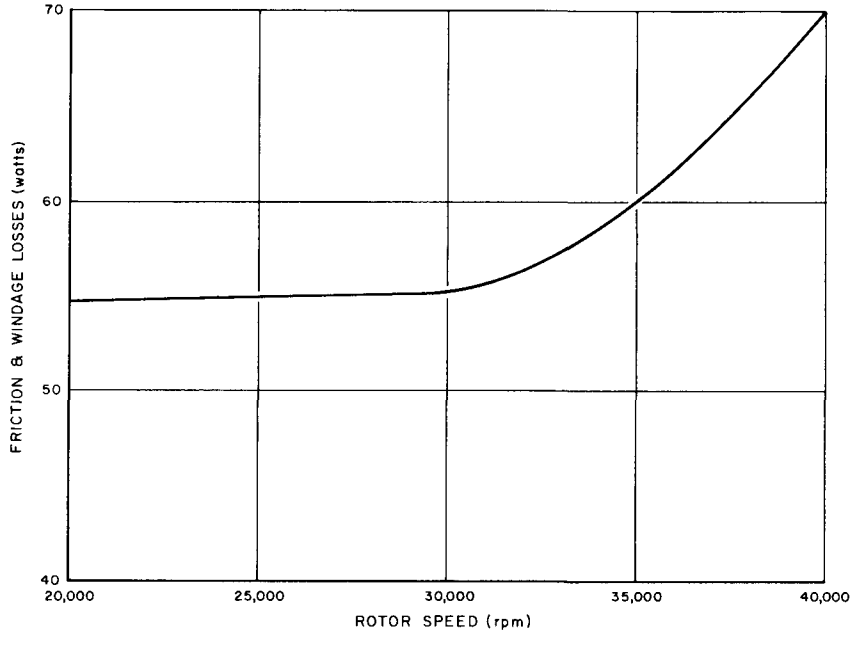

Figure 14. Combined Friction and Windage Losses of the Mark V Pump Rotor

VI. TEST RESULTS AND DISCUSSION

Comparative performance characteristics of the four radial gap rotating permanent magnet induction pump models are presented in Figures 15 and 16. Head-capacity curves are presented for each of the pumps. The test results are summarized in Table I. Because of the long periods between testing of the pumps, test conditions varied. Working fluid, maximum rotor speed, instrumentation, and ranges of test parameters were changed to correspond with changes in SNAP 2 system requirements, availability of improved materials and equipment, and need for additional test information.

TABLE I

SUMMARY OF RADIAL GAP ELECTROMAGNETIC PUMP TEST RESULTS

Test Pump	Weight (lb)	Fluid	Temperature (°F)	Rotor Speed (rpm)	Magnet Flux (gauss)	Maximum* Developed Pressure (psi)	Maximum Flow (gpm)
Mark I	5	Sodium	360	34,400	-	5.5	1.6
Mark II	8	Sodium	995	34,650	-	3.6	17.9
Mark III	4	Sodium	760	21,550	960	1.1	8.0
Mark III	4	NaK	790	21,550	960	0.6	3.9
Mark V	3	Sodium	1000	34,800	1400	8.4	8.1
Mark V	3	NaK	1000	40,000	1700	8.9	8.2

*Measured at zero flow

A. MARK I

The Mark I pump was tested at a maximum rotor speed of 34,400 rpm with sodium at 360°F. The test successfully demonstrated the feasibility of using the rotating permanent magnet induction pump for the SNAP 2 application. The steep decline of the head-capacity curve, however, indicated the need for improvement of the pump's hydraulic characteristics.

B. MARK II

The Mark II pump was tested at a maximum rotor speed of 34,650 rpm with sodium at 995°F. The design flow rate of this pump, 6.6 gpm of sodium, was

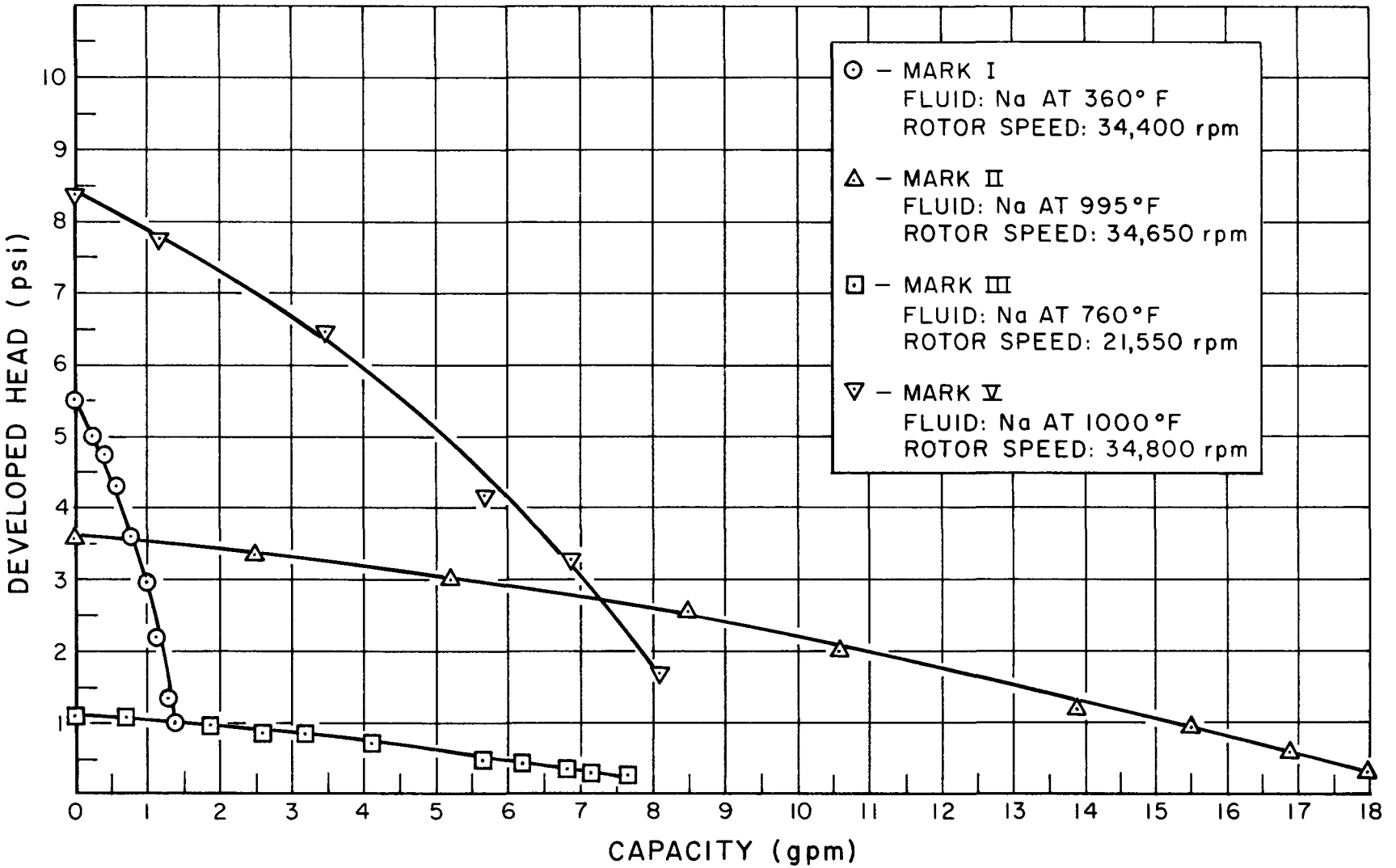

Figure 15. Comparative Performance Characteristics of Mark I, II, III, and V Pumps

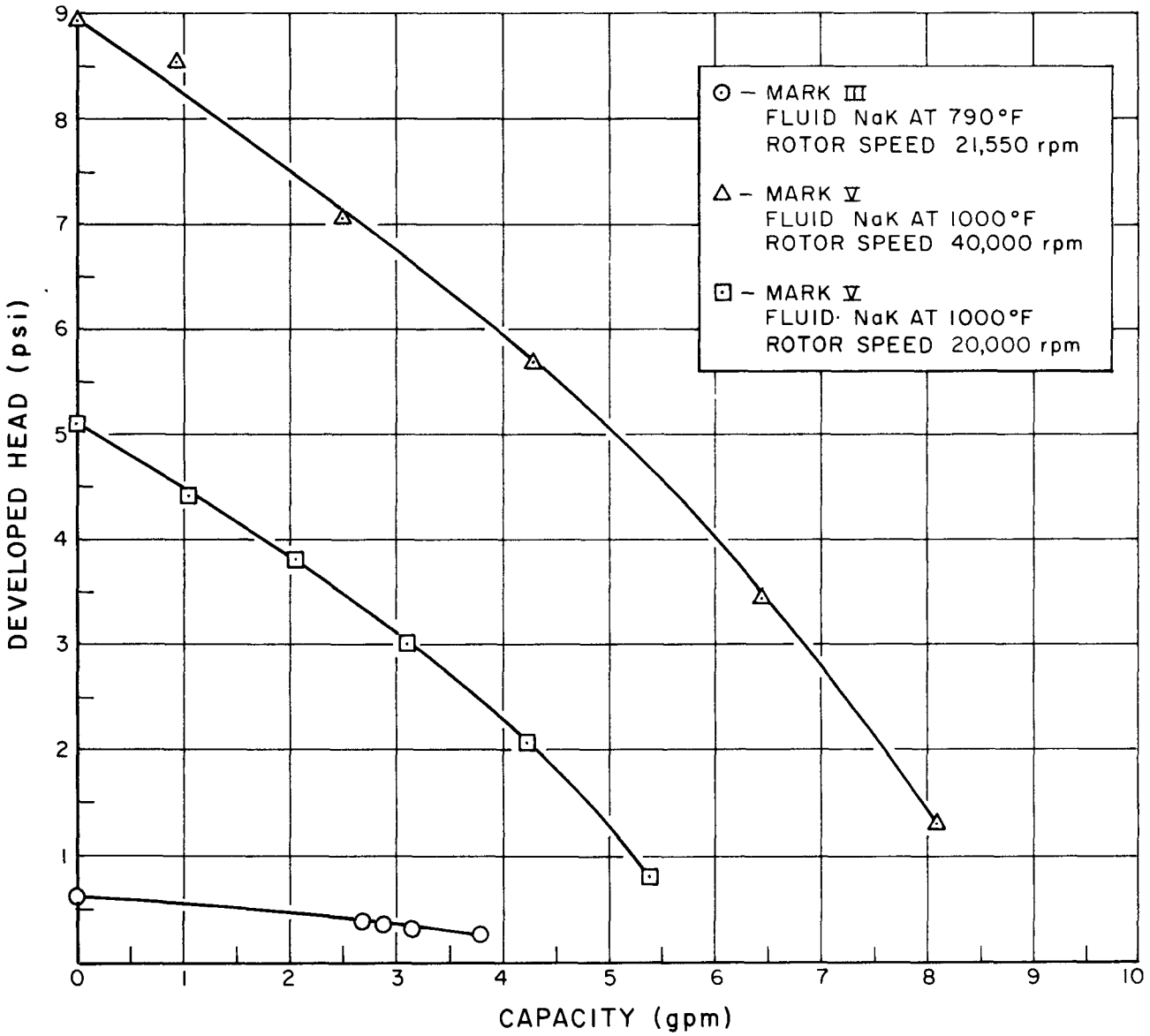

Figure 16. Comparative Performance Characteristics of Mark III and V Pumps

achieved with a developed pressure of 2.9 psi, slightly below the design point of 3 psi. The pump's hydraulic characteristics were satisfactory, but its weight of 8 pounds was excessive. This pump design clearly demonstrated that the radial gap pump concept has sufficient capability for the SNAP 2 system.

C. MARK III

The Mark III pump was tested at a maximum rotor speed of 21,550 rpm with sodium at 760°F and NaK at 790°F. This pump design represented an attempt to approach the SNAP 2 pump flow and weight requirements. The lengths of the magnet rotor assembly and the pumping section were made smaller than the Mark II pump components in order to reduce the pump weight.

The performance of this pump was below expectation. The calculated shutoff pressure was 2.4 psi compared to the experimental value of 1.1 psi obtained with sodium and with the short (1.15 in.) magnet length. The hydraulic and dynamic electromagnetic losses of this pump were relatively small; the difference between the shutoff pressure of 1.1 psi and developed pressure at maximum flow of 7.6 gpm was 0.85 psi. The maximum attainable rotor speed of 21,550 ppm was due to the rotor being slightly out of balance. Because of the poor pump performance, the rotor balance was not corrected.

Mark III was tested with both sodium and NaK to permit evaluation of the pumping characteristics of the NaK, which, having a higher resistivity (79×10^{-3} ohms at 1000°F compared to 29×10^{-3} at 1000°F) is more difficult to pump electromagnetically. The test results obtained with NaK circulated in place of sodium indicated a decrease in developed pressure at shutoff of 36%. The calculated decrease in shutoff pressure was 56%.

D. MARK IV

The Mark IV pump was not built because of design changes which led to the Mark V design.

E. MARK V

The Mark V pump exceeded the original SNAP 2 pump requirements of circulating 6.6 gpm of sodium at 3 psi developed pressure, temperature of 1000°F and pump weight of 3 pounds. With NaK as the coolant the pump performance was below design requirements, the experimental flow rate at 3 psi developed pressure was 6.8 gpm.

Mark V was tested over range of conditions as follows:

Working fluid	Na; NaK-78
Fluid temperature	700 to 1000°F
Rotor speed	10,000 to 40,000 rpm
Magnet flux	1400 to 1800 gauss

The head-capacity curves for various magnet flux levels with rotor speed as a parameter are shown in Figures 17 through 20. A comparison of the calculated head-capacity curve, which includes the measured hydraulic losses, with an experimental head-capacity curve is shown in Figure 21. Since the magnet flux density distribution in the air gap and the length of the induced current path in the liquid metal, factors affecting B_G and λ in the design Equation 1, are not amenable to precise determination, the agreement between the measured and predicted head-capacity curves can be deemed reasonable. The differences between the predicted developed pressures and the experimental values at the higher flow rates are attributed to the indeterminate braking action of the magnetic field upon the liquid metal. Figures 22 and 23 present a comparison of the experimental and calculated values of shutoff head as a function of rotor speed for both the Alnico V and Alnico VI magnets. The calculated shutoff pressures for both rotors at 40,000 rpm are $\sim$18% below the experimental values. The percentage variation over the rotor speed range of 15,000 to 40,000 rpm remains fairly constant. The experimental head-capacity curves obtained at constant rotor speed of 40,000 rpm with temperature as a parameter are shown in Figure 24. The effect of temperature should be mainly due to the changed resistivity of the NaK-78. This is borne out by a comparison of the experimental shutoff heads as a function of temperature and the calculated values shown in Figure 25; the slopes of the two curves are approximately equal.

The efficiencies of the Mark V pump, tested with the several magnet-rotor assemblies, are presented in Figure 26 as a function of the pump capacity. The peak efficiency, 2%, was obtained at slightly less than one-half of design flow. The efficiencies under space conditions will be slightly higher since windage losses will be greatly reduced. The lower efficiency of the pump with the Alnico VI magnet rotor assembly was due to a small imbalance of the rotor which increased the friction losses. The variation of efficiency with rotor speed is shown in Figure 27. The peak efficiency, 2.2%, was reached with a rotor speed of 30,000 rpm.

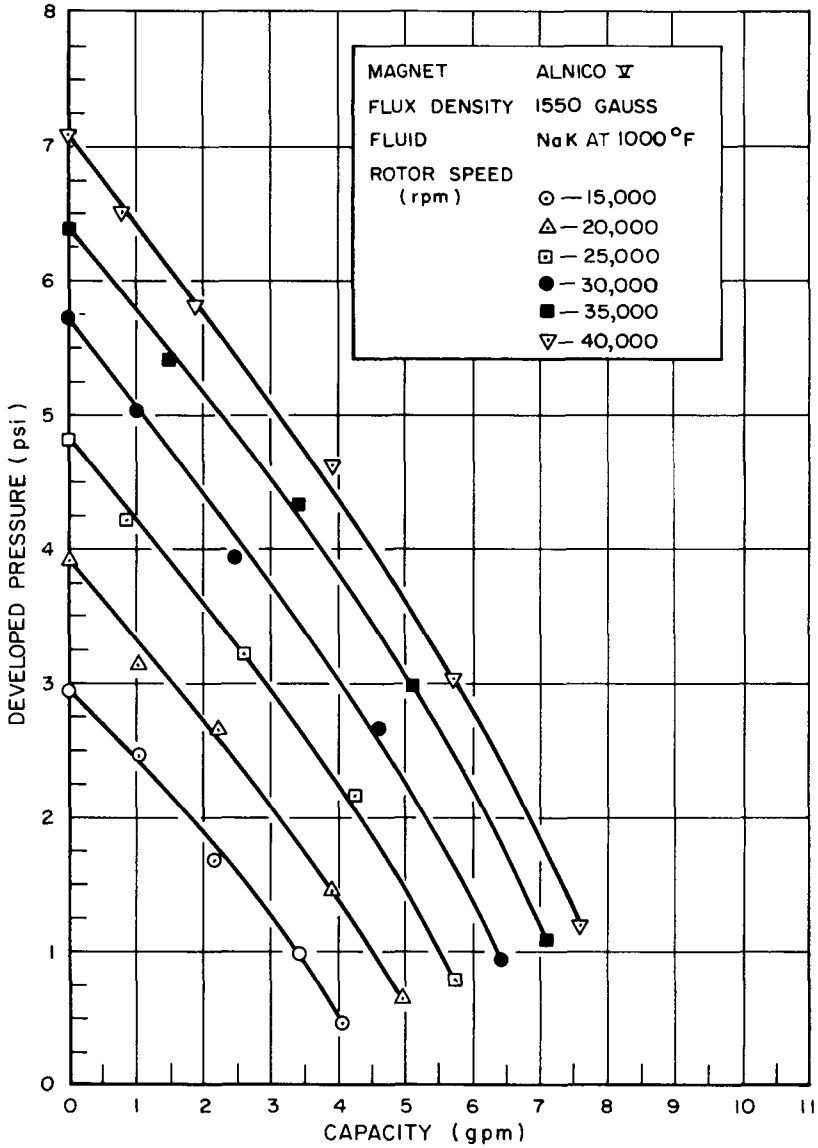

Figure 17. Performance Characteristics of Mark V Pump: B = 1550 Gauss

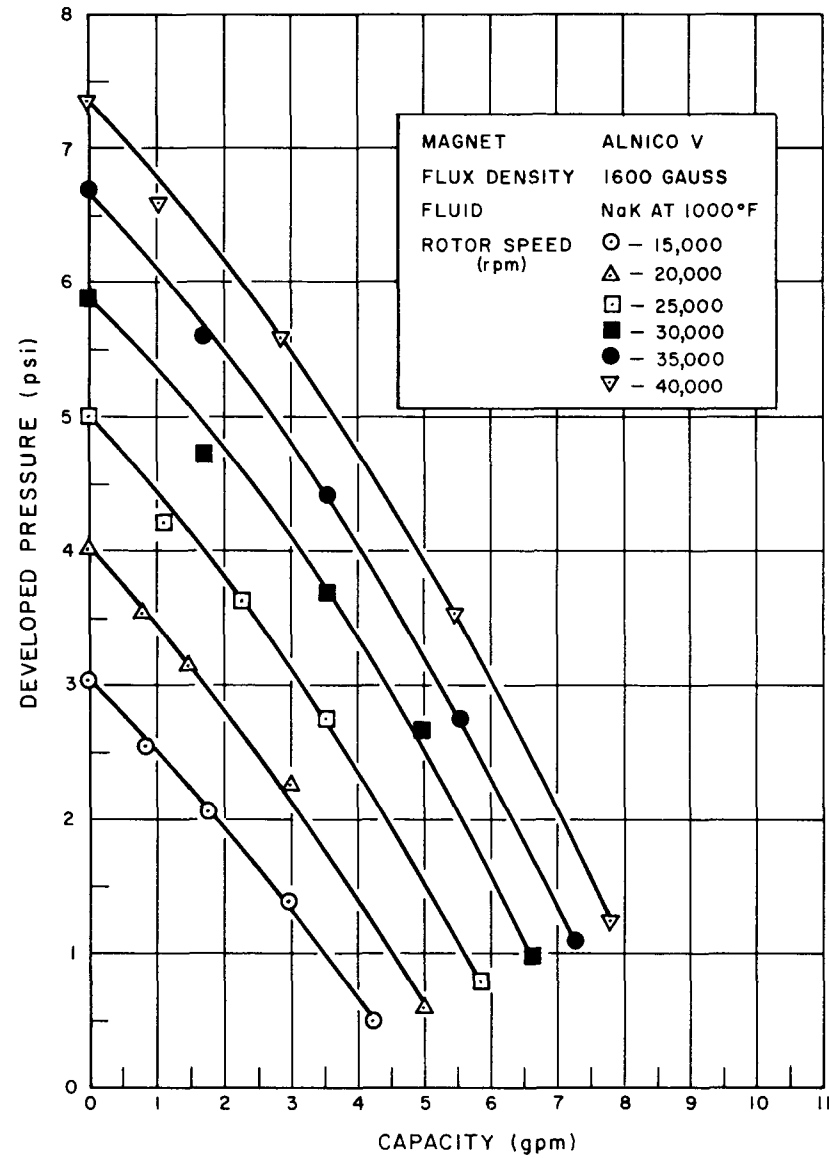

Figure 18. Performance Characteristics of Mark V Pump: B = 1600 Gauss

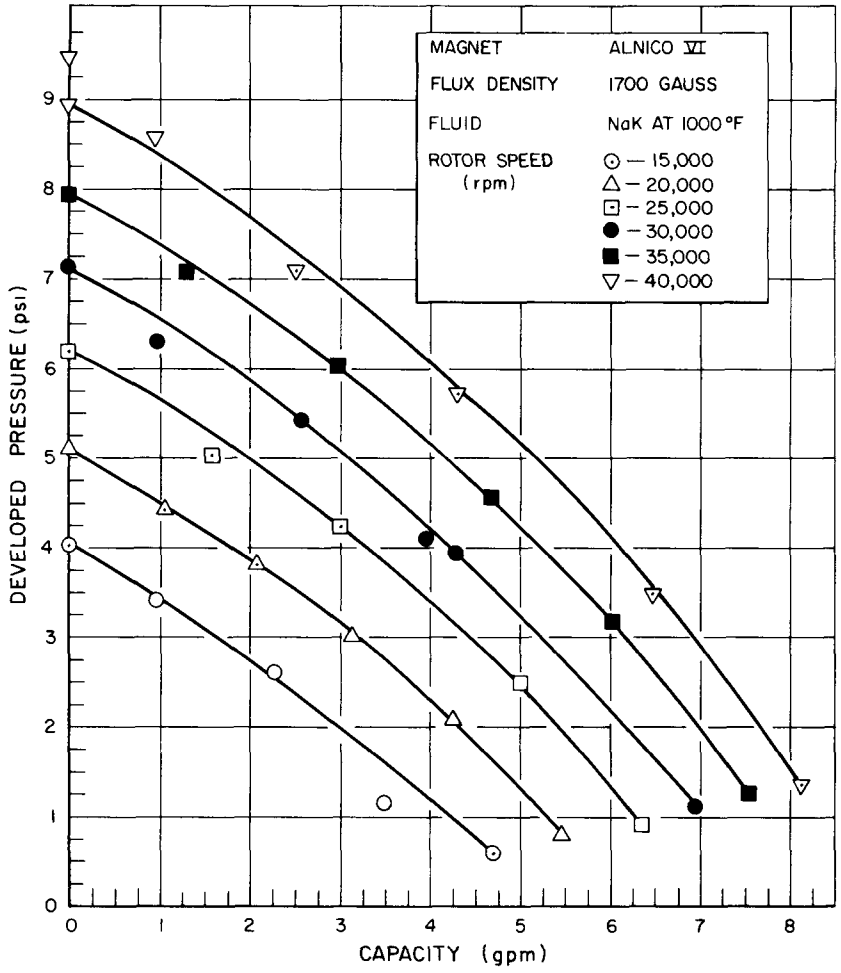

Figure 19. Performance Characteristics of Mark V Pump: B = 1700 Gauss

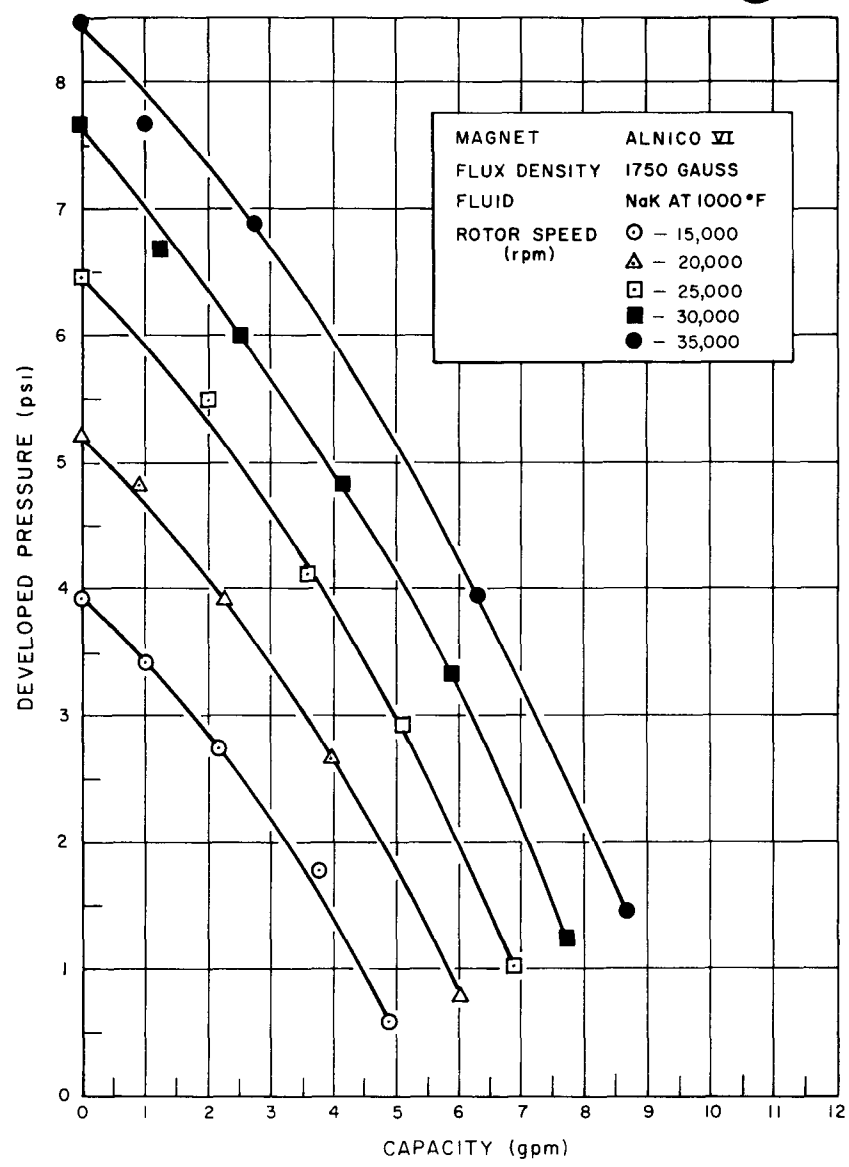

Figure 20. Performance Characteristics of Mark V Pump: B = 1750 Gauss

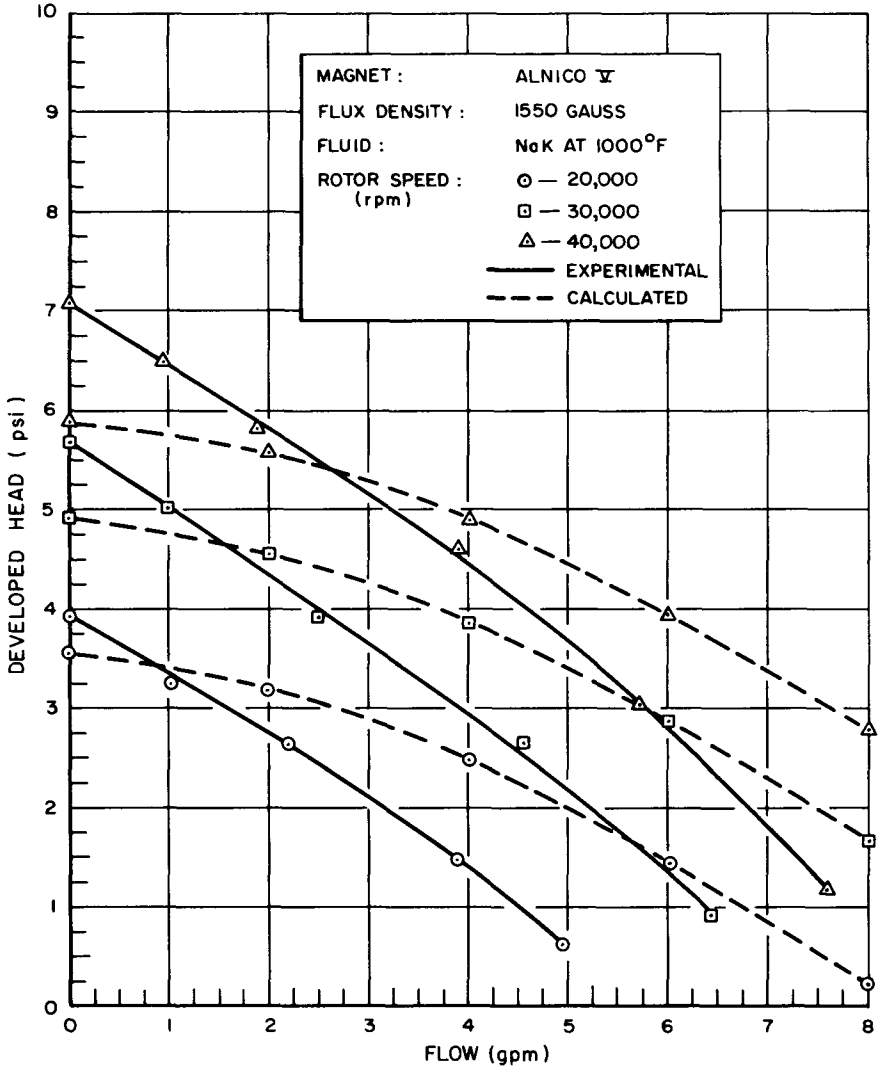

Figure 21. Comparison of Experimental and Calculated Performance Characteristics of Mark V Pump

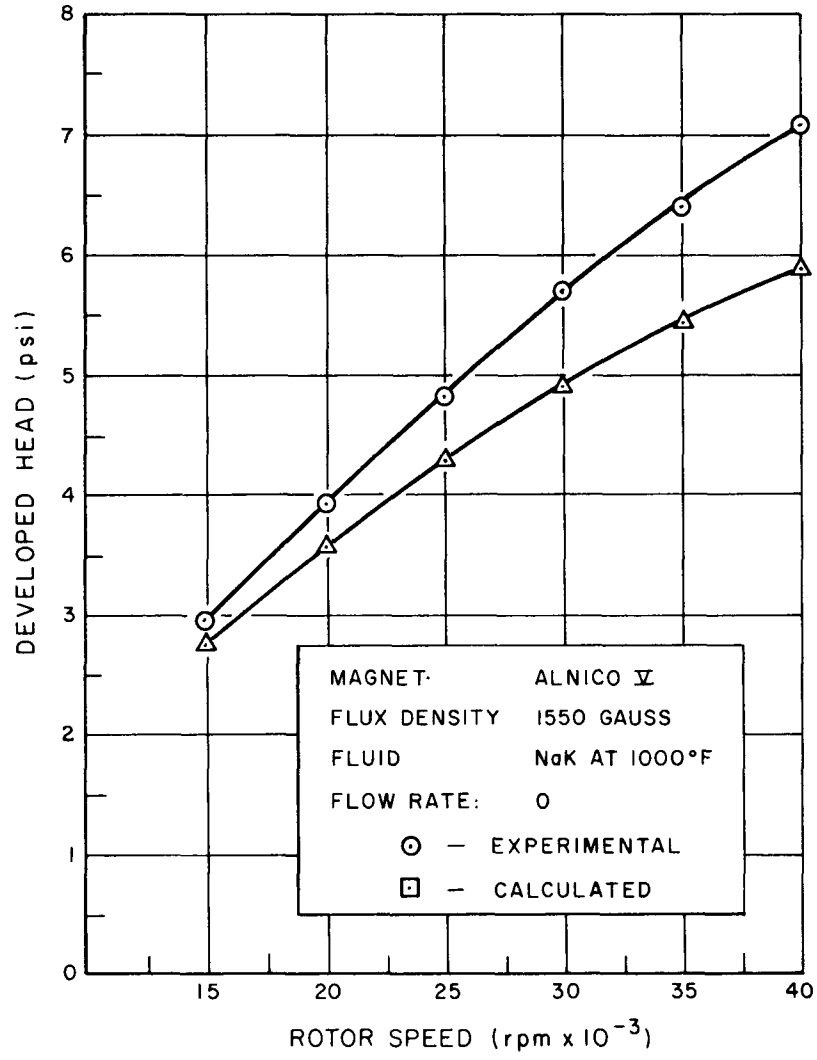

Figure 22. Comparison of Experimental and Calculated Developed Pressures for the Mark V Pump at Shutoff: B = 1550 Gauss

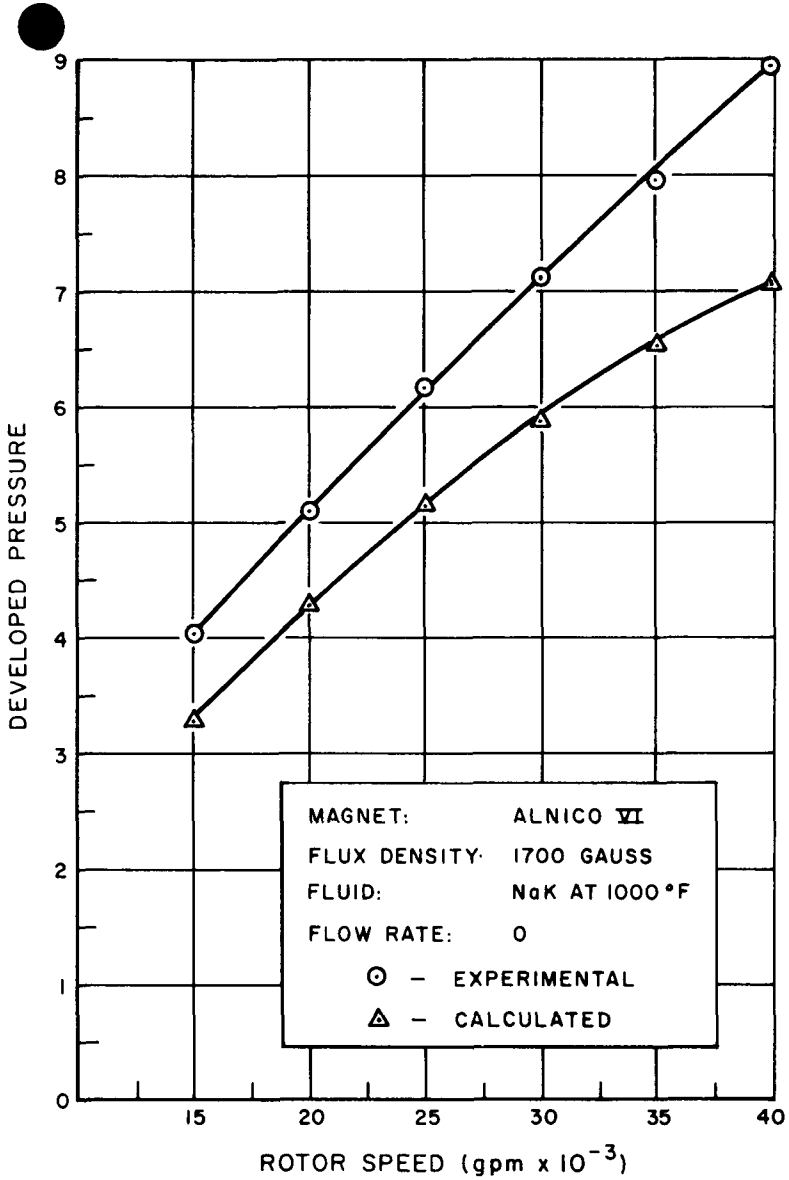

Figure 23. Comparison of Experimental and Calculated Developed Pressures for the Mark V Pump at Shutoff: B = 1700 Gauss

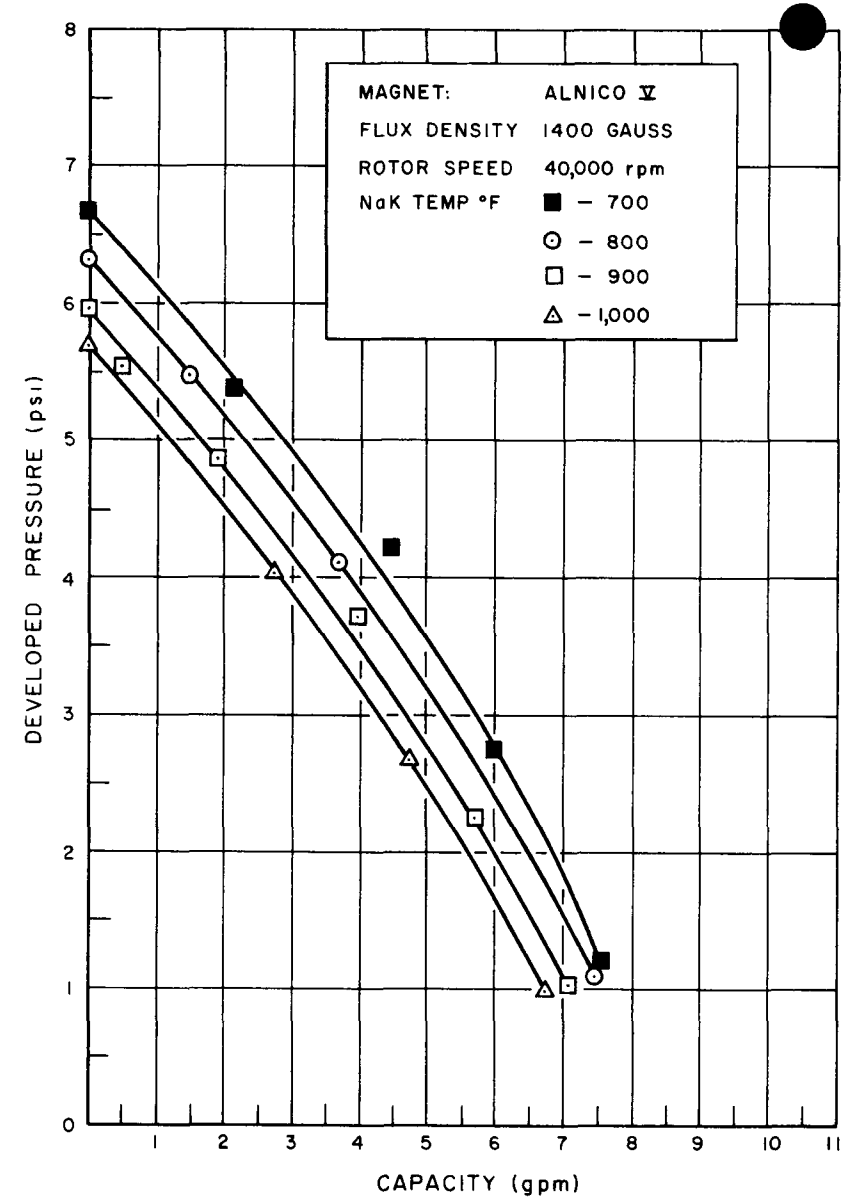

Figure 24. Mark V Pump: Effect of Temperature on Head-Capacity Characteristics

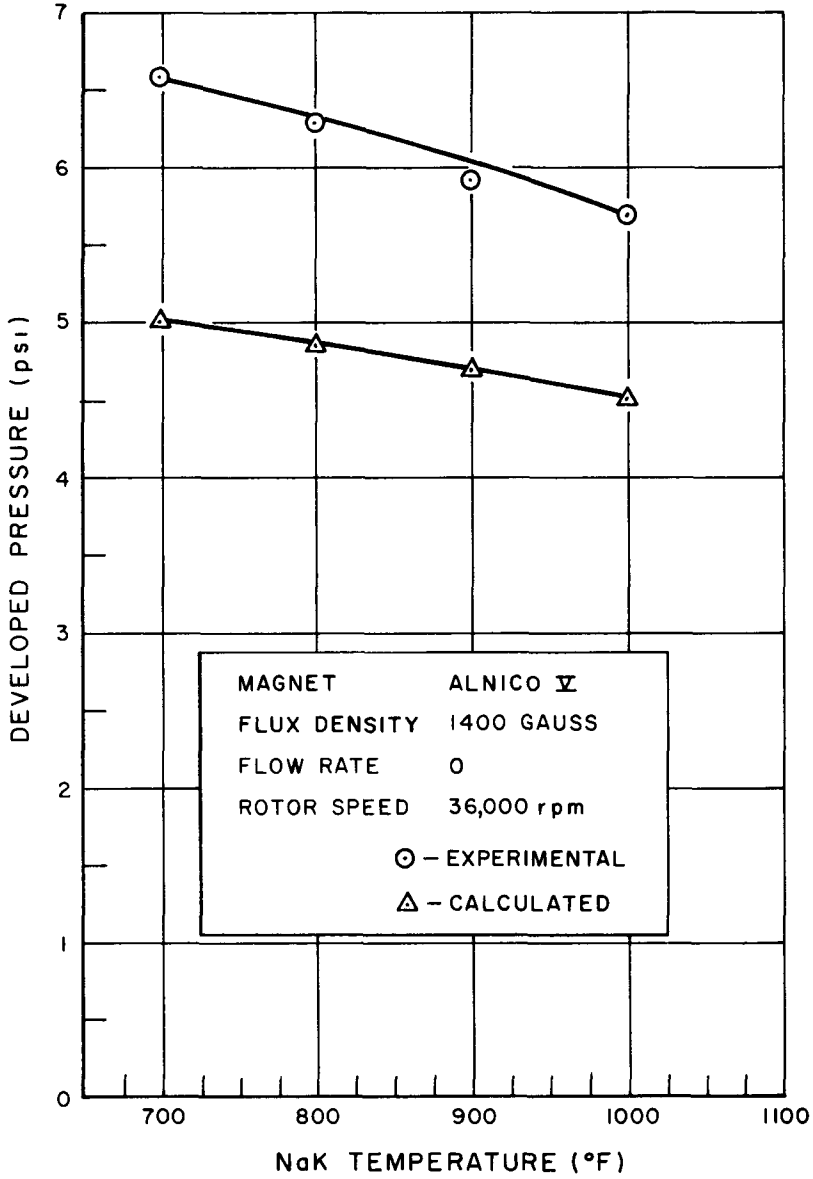

Figure 25. Mark V Pump: Comparison of Experimental and Calculated Effect of Temperature

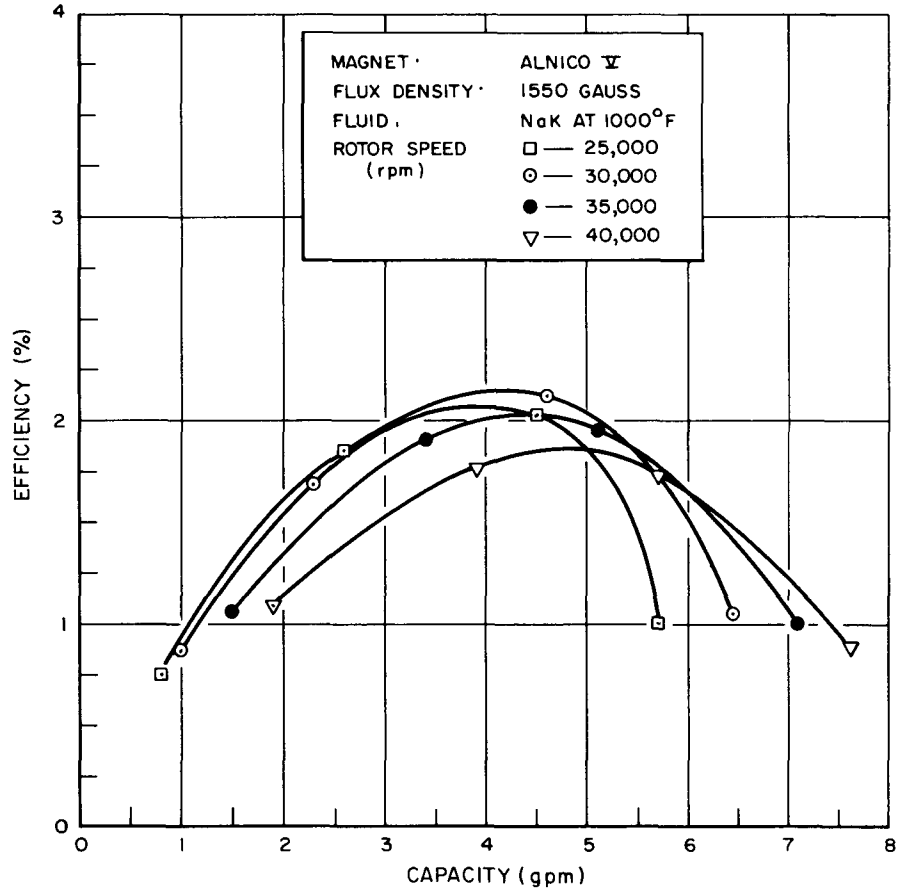

Figure 26. Mark V Pump: Efficiency vs Flow and Rotor Speed

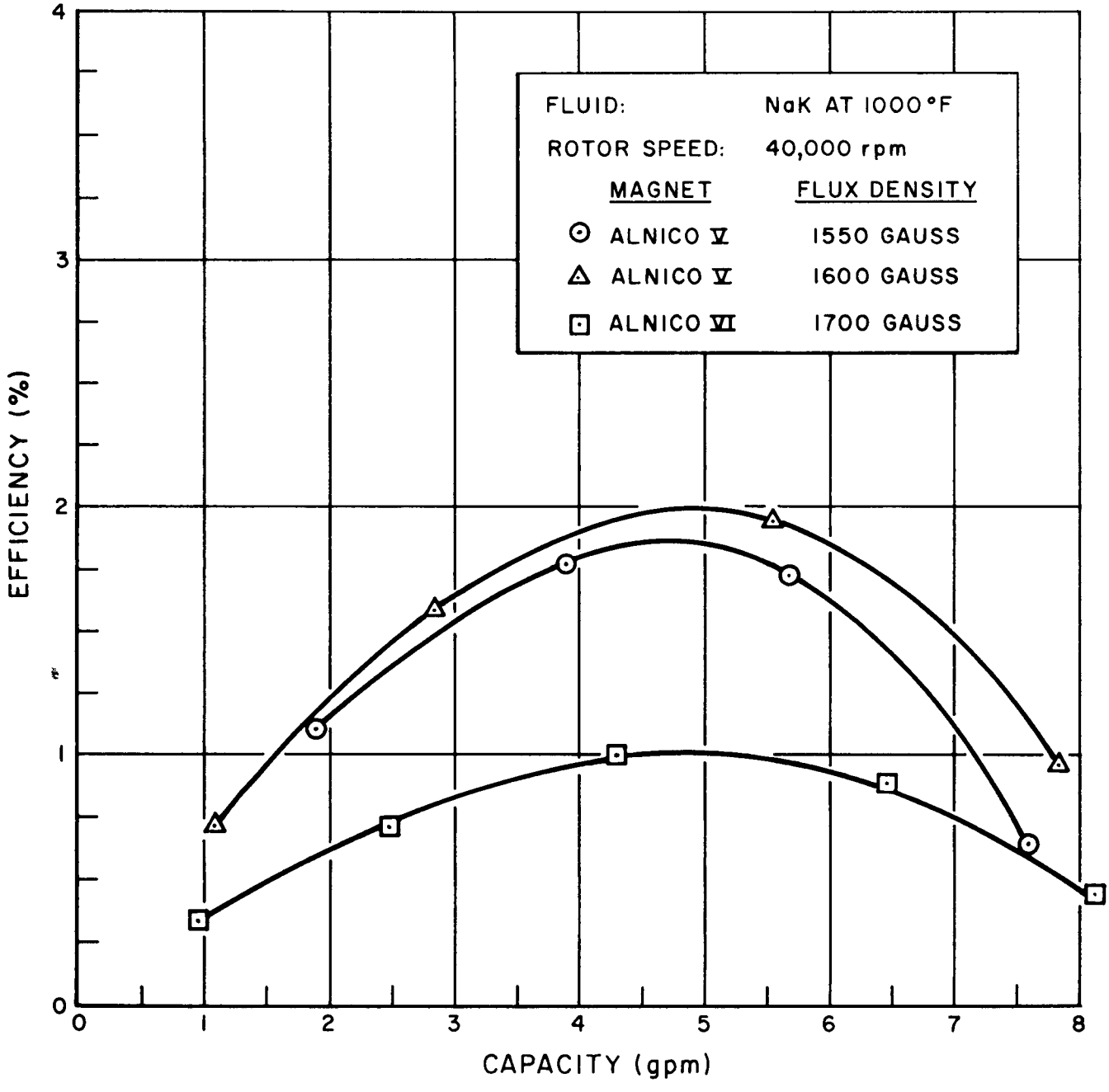

Figure 27. Mark V Pump: Efficiency vs Flow and Magnet Flux

VII. CONCLUSION

The radial gap permanent-magnet pump is capable of circulating 1000°F sodium or NaK at magnet rotor speeds as high as 40,000 rpm with reasonable efficiency. The simplicity of design, essentially a helically coiled tubular pumping duct mounted coaxial to the rotating cylindrical magnet which acts as an inductive power source and permits complete containment of the liquid metal, affords a high degree of reliability making the Mark V pump design suitable for application to SNAP reactor systems utilizing NaK coolant. The agreement obtained between the experimentally determined pump performance characteristics and the design predictions plus the demonstrated capability of the radial gap pump indicate that a pump which will meet the SNAP 2 requirements can be produced with little further development work.

APPENDIX A
SAMPLE CALCULATIONS

A. THEORETICAL PRESSURE DEVELOPED BY THE MARK V PUMP

System parameters for the case of circulation of 1000°F NaK with rotor speed of 40,000 rpm at zero flow were as follows:

$$V_{syn} = \frac{2\tau(n)}{60} = 9360 \text{ cm/sec}$$

λ = 3.60 cm (average length of pumping section)

τ = 7.03 cm

δ = 0.660 cm

δ_1 = 0.508 cm

B_A = 1550 gausses; $B_G = \frac{\pi}{2} B_A$

$\rho = 76.9 \times 10^3$ abohm-cm.

Conversion factor: 1 psi = 68,944 dynes/cm^2

$$P = \frac{V_{syn} \lambda B_G^2}{2\rho(68,944)} \left\{ \frac{\frac{\lambda}{\tau} + \frac{\tau}{\lambda}}{\left[\frac{4V_{syn}\delta_1\lambda}{\rho\delta}\right]^2 + \left[\frac{\lambda}{\tau} + \frac{\tau}{\lambda}\right]^2} \right\}$$

P = 5.87 psi.

B. CALCULATED DEVELOPED PRESSURE UNDER FLOW CONDITIONS

$$P_{net} = P - P_{axial} - P_{hydraulic}$$

System parameters as in (A) except for flow rate

Flow rate = 6 gpm

V_1 = 696 cm/sec

$V_{1a} = V_1 \tan\theta$ = 99.4 cm/sec

1. $$P = \frac{(V_{syn} - V_1)\lambda B_G^2}{2\rho(68,944)} \left\{ \frac{\frac{\lambda}{\tau} + \frac{\tau}{\lambda}}{\left[\frac{4(V_{syn} - V_1)\delta_1\lambda}{\rho\delta}\right]^2 + \left[\frac{\lambda}{\tau} + \frac{\tau}{\lambda}\right]^2} \right\}$$

$P = 5.81$ psi

2. $$P_{axial} = \frac{V_{1a}\tau B_G^2}{2\rho(68,944)} \frac{\frac{\lambda}{2\tau} + \frac{2\tau}{\lambda}}{\left[\frac{4V_{1a}\delta_1}{\rho\delta}\right]^2 + \left[\frac{\lambda}{2\tau} \quad \frac{2\tau}{\lambda}\right]^2}$$

$P_{axial} = 2.04$ psi

3. $P_{hydraulic}$ (from Figure 12)

$P_{hyd} = 3.0$ psi

$\therefore P_{net} = 2.77$ psi.

NOMENCLATURE

B_A = average value of magnetic flux, gausses

B_G = maximum value of magnetic flux, gausses

D = equivalent diameter of pump duct

E_A = induced emf, volts

f = friction factor for flow through a tube

g = acceleration of gravity, ft/sec^2

h = circumference of pump duct measured along centerline, cm/sec

l = length, cm

L_m = magnet diameter, cm

n = rotor speed, rpm

P = pressure rise across pump, psi

P_{axial} = electromagnetic pressure loss, psi

$P_{hydraulic}$ = hydraulic pressure loss, psi

ΔP_m = pressure drop in liquid metal system

ΔP_w = pressure drop in water system

Q = flow rate, gal/min

v = field velocity, cm/sec

V = fluid velocity, ft/sec

V_l = liquid velocity along centerline of stream in a direction tangent to the centerline and normal to the axis

V_{syn} = field velocity along centerline of stream, cm/sec

W_i = power input, watts

W_o = power output, watts

δ = radial air-gap, cm

δ_l = internal width of pump duct, cm

λ = axial length of electrical conduction path in pump direct, cm

η = efficiency

ρ = electrical resistivity of liquid metal, abohm-cm; density, lb/cu-ft

τ = pole pitch measured along centerline of pump duct, cm

BLANK

REFERENCES

1. B. A. Snoke and J. Tiltins, The SNAP 2 Power Conversion System Topical Report No. 10, "Sodium Pump Design and Testing," TRW-ER-4106, August 5, 1960.
2. R. Rudenberg, "Analysis of an Eddy Current Device," Report to the Allis-Chalmers Mfg. Company, Order No. WA-467351-7670, August 20, 1949.
3. R. S. Baler, "Calculation of Developed Pressure and Fluid Power in Linear Polyphase Induction Liquid Metal Pumps," Mine Safety Appliance Co., Technical Report 48, Contract NObs-65426, Index No. NS-200-021, March 24, 1956.
4. R. Rudenberg, "Sammlung Elektrotechnischer Vortrage," Verlag Enke Von Ferdinand, Stuttgart, Germany, Band 10, p. 269-370, 1907.
5. J. F. Asti, "Development of Electromagnetic Pumps for Liquid Metals," Allis-Chalmers Mfg. Company, Atomic Power Section, Report No. 43-109, Contract NObs-47750, Index No. WA-643-049, p. 13, Appendix E, June 30, 1952.
6. Personal communication from R. L. Wallerstedt, Atomics International.
7. J. K. Vennard, "Elementary Fluid Mechanics," 3rd Ed., Chapter 8, John Wiley and Sons, New York, 1956.